Scientific Reports

https://doi.org/10.1038/s41598-026-46483-0

Article in Press

Performance assessment of a novel citrus-based biopolymer for enhanced oil recovery in harsh reservoir conditions– an experimental study

Received: 6 January 2026

Accepted: 26 March 2026

Published online: 03 April 2026

Cite this article as: Ali A.G., Amao A.M., Altawati F.S. *et al.* Performance assessment of a novel citrus-based biopolymer for enhanced oil recovery in harsh reservoir conditions– an experimental study. *Sci Rep* (2026). https://doi.org/10.1038/s41598-026-46483-0

Ammar G. Ali, Abiodun M. Amao, Faisal S. Altawati & Taha M. Moawad

Performance Assessment of a Novel Citrus-Based Biopolymer for Enhanced Oil Recovery in Harsh Reservoir Conditions – An Experimental Study

Ammar G. Ali [1], Abiodun M. Amao[1,] *, Faisal S. Altawati [1], Taha M. Moawad [1]

[1] Department of Petroleum and Natural Gas Engineering, College of Engineering, King Saud University, P.O. Box 800, Riyadh, Saudi Arabia.

* Corresponding author: *aamao@ksu.edu.sa*

Abstract

The growing demand for energy and stricter environmental regulations necessitate the adoption of sustainable oil recovery methods, particularly in high-salinity, high-temperature (HSHT) reservoirs, where conventional synthetic polymers often suffer from viscosity loss, thermal degradation, and precipitation. This study evaluated a novel biopolymer extracted from orange peel waste as a cost-effective and environmentally benign alternative for polymer flooding under HSHT conditions. The biopolymer was produced through an optimized extraction process and characterized in terms of viscosity, thermal stability, and interfacial properties. Core flooding experiments were performed on Berea and Saq sandstone cores at 90 °C and 165,000 ppm salinity under three injection scenarios: conventional waterflooding (base case), polymer injection immediately after water breakthrough (W_{BT}), and early polymer injection before significant water production. Citrus-based biopolymer maintained adequate viscosity at reservoir temperature and reduced oil–water interfacial tension from 21.8 to 8.59 mN/m; however, the primary recovery mechanism for the present formulation is mobility control rather than ultralow-IFT mobilization. In Berea sandstone, ultimate oil recovery increased from 47.6% in the base case to 51.7% and 63.35% when polymer was injected after W_{BT} and at an early stage, respectively. For Saq sandstone, early polymer injection increased final oil recovery from 46.2% to 70.3% relative to the base case. These results correspond to incremental gains of approximately 15.8 and 24.1 percentage points of OOIP relative to the respective base-case

waterfloods in Berea and Saq cores. Overall, the findings demonstrated that citrus-derived biopolymers would address key limitations of conventional polymers in HSHT reservoirs while valorizing an abundant agricultural waste stream and supporting circular-economy principles.

Keywords: Sustainable EOR, Polymer Flooding, EOR Biopolymer, Waste Materials, Valorization of Citrus Waste.

1. Introduction

Enhanced oil recovery (EOR) techniques have become increasingly crucial in the petroleum industry as easily accessible oil reserves become increasingly scarce. These methods aim to extract additional oil from reservoirs beyond what is achievable through conventional recovery methods (Green and Willhite 2018). In recent years, there has been a growing emphasis on using green materials in EOR processes to enhance sustainability and minimize environmental impact while maintaining or improving recovery efficiency.

Oil recovery typically occurs in three phases, each characterized by distinct mechanisms and recovery efficiencies. Primary recovery, which relies on natural reservoir energy, typically yields 5–15% of the original oil in place (OOIP) (Muggeridge et al. 2014). Secondary recovery methods, involving the injection of water or gas, can recover an additional 20–40% of OOIP (Sheng 2011). Tertiary recovery, or EOR, employs various techniques to alter reservoir or fluid properties, potentially recovering an additional 10-30% of OOIP (Alvarado and Manrique 2010). Chemical EOR methods have consistently outperformed other EOR techniques. These chemical methods include polymer flooding, surfactant flooding, alkaline flooding, and their combinations. While polymer-based chemical EOR has proven successful in numerous projects, the reliance on synthetic polymers, particularly hydrolyzed polyacrylamide (HPAM) (Standnes and Skjevrak 2014), poses significant environmental concerns. The detrimental effects of HPAM on soil, surface and underground waters, and overall environmental health have raised significant concerns. One notable example is the Daqing field

in China, where large-scale polymer flooding was implemented in 1996, and polymer flooding constituted 23% of the overall oil production in December 2017 (Jiexun et al., 2019).

However, the problem with synthetic polymers is not just an environmental issue; acrylamide-based polymers are susceptible to degradation under elevated temperatures and high-salinity conditions, primarily due to the hydrolysis of amide and side groups, resulting in polymer precipitation. This hydrolytic process is contingent upon a specific concentration of divalent ions (Ca^{2+}, $Mg^{2+)}$ in hard saline brines. Additional degradation mechanisms include reactions with dissolved oxygen and scission of the carbon-carbon backbone. Consequently, widely utilized synthetic polymers such as HPAM exhibit poor thermal and mechanical stability under harsh reservoir conditions, as their viscosity decreases markedly with increasing temperature. This degradation manifests as a reduction in viscosity and thermal stability, leading to polymer precipitation and retention within the porous media. Such phenomena necessitate the excessive application of chemicals, potentially exacerbating environmental impact. These limitations significantly compromise the efficacy of these polymers in challenging reservoirs, as demonstrated by several experimental and field studies on HPAM performance under HSHT and hard-brine conditions(Jang et al. 2015; Seright et al. 2020; Gbadamosi et al. 2022a). Nevertheless, the limitations of polyacrylamide-based synthetic polymers in high-salinity, high-temperature environments can be mitigated using copolymers. Enhanced thermal stability is achieved by incorporating monomers, such as 2-acrylamide-tertiary-butyl sulfonic acid (ATBS), AMPS (2-acryl amido-2-methyl propane sulfonic acid), and NVP (n-vinylpyrrolidone) (Levitt and Pope 2008; Gaillard et al. 2010; Vermolen et al. 2011; Dupuis et al. 2017). Additional innovative solutions include the development of thermo-responsive polymers (Chen et al. 2013; Li et al. 2017, 2019; Xie and Liu 2017; Divers et al. 2018) and salt-induced polymers (Li et al. 2019). However, environmental concerns persist and must be addressed with alternatives to synthetic chemical-based polymers.

The global challenge of meeting energy demands while maintaining environmental responsibility drives research into eco-friendly materials for enhanced oil recovery. These environmentally friendly alternatives include biopolymers, biosurfactants, and plant-derived alkaline agents, which have shown promising results in laboratory and field trials. Developing and applying these green materials in chemical EOR processes represents a significant opportunity for improving the sustainability of oil recovery operations while maintaining economic viability.

The history of using green materials in EOR through polymer flooding or surfactant flooding has evolved significantly over the years, driven by the need for environmentally friendly, cost-effective, and efficient alternatives to synthetic polymers. Initially, synthetic polymers like HPAM were widely used due to their effectiveness in improving sweep efficiency and reducing the water-oil mobility ratio (Al Nabhani et al. 2024; Southwick et al. 2024). However, concerns over the high cost and environmental impact of synthetic polymers and surfactants have led to increased research into natural and green materials. Green or biomaterials in EOR present significant ecological benefits, primarily due to their biodegradability, non-toxicity, and reduced environmental footprint compared to conventional synthetic polymers.

Green polymers in EOR refer to environmentally friendly polymers that improve oil recovery while minimizing environmental impact. The integration of green polymers in EOR processes also aligns with the principles of green chemistry, which emphasizes the use of non-polluting and degradable materials derived from natural sources to minimize environmental impact (Elsayed Abdel-Raouf et al. 2022). Diverse biopolymers have been explored as potential replacements for synthetic polymers in EOR applications. These include, but are not limited to, Xanthan gum (Standnes and Skjevrak 2014; Jang et al. 2015; Sveistrup et al. 2016; Tackie-Otoo et al. 2020; Clinckspoor et al. 2021), Scleroglucan (Davison and Mentzer 1982; Sveistrup et al. 2016; Clinckspoor et al. 2021), Schizophyllan (Sveistrup et al. 2016; Gao 2016; Clinckspoor et al. 2021), Starch (Sveistrup

et al. 2016), Welan gum (Gao 2015), Terrestrial mushroom (Tengku Mohd et al. 2020), polymtea (Moawad et al. 2007), extracted mucilage from hollyhocks, Alcea, seeds (Nowrouzi et al. 2020), molasses from okra, Abelmoschus Esculentus, (Gbadamosi et al. 2022b) , Guar gum (Clinckspoor et al. 2021) and more recently, a citrus-based biopolymer (Ali et al. 2024) and pomegranate peel-derived biopolymer (Ali et al. 2025)

Despite these diverse alternatives, only Xanthan gum and Schizophyllan have been deployed in oilfield EOR operations. A comprehensive study by Standnes and Skjevrak (Standnes and Skjevrak 2014) highlighted the limited adoption of biopolymers, revealing that they were employed in a mere 8% of polymer-based EOR projects conducted over a 50-year timeframe from 1964 to 2014. Xanthan gum and guar gum, both natural polymers, have shown promising results in EOR applications due to their high resistance to challenging reservoir conditions, including high salinity and temperature, which are common in oil recovery processes (Musa et al. 2021; Obuebite and Okwonna 2023). The use of biopolymers like guar gum grafted with acrylamide and 2-acrylamide-2-methylpropane sulfonic acid (AMPS) has proven effective in high-salinity reservoirs, showcasing their potential to replace synthetic polymers like partially HPAM, which are non-biodegradable (Elsaeed et al. 2021).

The application of green polymeric nanoparticles, such as those derived from eucalyptus and walnut shells, has improved oil recovery by altering interfacial tension (IFT) and wettability, thereby enhancing the efficiency of the EOR process while being environmentally benign (Ahmadi et al. 2023). Core flooding experiments using green polymers have shown promising results in enhancing oil recovery while addressing environmental concerns associated with synthetic polymers.

Several studies have investigated the effectiveness of various natural and eco-friendly polymers. For instance, Abelmoschus esculentus, a natural polymer, improved oil recovery by 16.26% in oil-wet sandstone cores (Obuebite and Okwonna 2023). Gbadamosi et al. (Gbadamosi et al. 2022b)

studied the potential of okra mucilage for EOR in carbonate cores under high-temperature and high-pressure (HTHP) conditions. The results showed an additional oil recovery of 12.7% compared to waterflooding methods, demonstrating its effectiveness in improving oil displacement. Similarly, local polymers, such as Afzelia africana and Colocasia esculenta, have shown promising results, with oil recoveries comparable to synthetic polymers, highlighting their potential as cost-effective and eco-friendly alternatives (Ekene et al. 2024). Schizophyllan, derived from local sources in Malaysia, exhibited shear-thinning behavior and maintained its viscosity even after aging at high temperatures, resulting in an incremental oil recovery of 17.25% in core flooding experiments (Gunaji et al. 2022). Additionally, Aadland et al. (Aadland et al. 2019) studied cellulose nanocrystals (CNC), which are derived from natural sources such as wood pulp, making them renewable and biodegradable; CNC showed potential in EOR applications, with a core flood experiment at 120 °C resulting in a total oil recovery of 62.2%, attributed to the formation of local log-jams within the porous media. More recently, Ali et al. (Ali et al. 2025) investigated experimentally the use of pomegranate peel-derived biopolymer as a sustainable EOR agent, demonstrating that a 7% solution achieves 62.2% ultimate oil recovery through mobility control under high-temperature and high-salinity reservoir conditions.

The use of Xanthan gum in combination with other green surfactants like alkyl polyglycoside (APG) has demonstrated significant improvements in oil recovery from sandstone reservoirs while maintaining environmental safety, while their applicability in carbonate reservoirs remains under investigation (Haq 2021b, a). Additionally, the development of green alkali-surfactant-polymer (ASP) formulations, such as those incorporating monoethanolamine (MEA), sodium cocoyl alaninate (SCA), and Schizophyllan (SPG), has been shown to mitigate surfactant precipitation and scale formation, while offering better oil recovery rates and reducing environmental hazards compared to conventional ASP formulations (Tackie-Otoo et al. 2022). Another study (Jiang et al. 2024) discussed an innovative use of polyformaldehyde glycol ether polymer

(PGEP) as a surfactant in oilfield development, where it is simple to synthesize, easily biodegradable, green, and environmentally friendly. It demonstrates alignment with current trends in oil and gas development, meeting stringent environmental regulations while achieving high oil recovery efficiency and low IFT. Ahmadi et al. (Ahmadi et al. 2023) investigated the use of green polymeric nanoparticles like Xanthan/magnetite/SiO_2 nanocomposites (NC), eucalyptus plant nanocomposites (ENC), and walnut shell nanocomposites (WNC) for EOR applications in carbonate reservoirs. The study demonstrated that ENC and WNC significantly enhanced IFT reduction and altered wettability, resulting in higher oil recoveries in carbonate reservoirs. Moreover, Qi et al. (Qi et al. 2023) found that using green materials extends beyond polymer flooding or surfactants in EOR processes. It was found that the use of the biodegradable polymer poly-L-proline as a green inhibitor prevents gas hydrate formation in oil-water systems, while reducing the concentration of dissolved gases, thereby preventing environmental contamination.

The comprehensive literature reviews presented critical limitations of current EOR technologies. Conventional synthetic polymers like HPAM suffer from severe degradation and precipitation in HSHT conditions, while existing biopolymers such as Xanthan gum and guar gum, despite their promise, face thermal stability challenges. Although some alternatives like Schizophyllan demonstrate better thermal stability, their high production costs limit commercial viability. These identified gaps in current technology, particularly for Middle East reservoirs characterized by HSHT conditions, drive the present research into citrus peel waste-derived biopolymers as a potential solution. Adopting green polymers and surfactants in EOR operations would increase oil recovery efficiency and significantly reduce environmental impact, making them a sustainable alternative to conventional synthetic polymers. The shift towards green materials in EOR processes reflects a broader trend of adopting sustainable and efficient technologies to meet the dual challenges of economic viability and environmental stewardship in the oil industry.

In this study, the potential of a novel citrus-based biopolymer as a sustainable and cost-effective alternative for EOR in harsh reservoirs was investigated experimentally. Systematic core flooding experiments under simulated HSHT conditions of 90 °C and 165,000 ppm salinity were conducted. Core flooding experiments were conducted on two different sandstone core samples (Berea and Saq core samples) to investigate the viability of the biopolymer and the impact of injection timing, comparing early polymer injection with conventional late injection scenarios, where the experiments analyzed the sweep efficiency and oil displacement capabilities.

2. Experimental Materials and Methods

2.1 Materials

2.1.1 Polymer solution

The biopolymer was extracted from orange peels through a multi-step process. Local fresh navel oranges were used, and their peels were separated into whole peels and albedo (the inner white part). These peels were dried in an oven for 24 hours at 70°C, then crushed to a size of 1–2 cm, and a portion was further ground into a powder. The powdered peels are then mixed with distilled water (DW), seawater (SW), 50% diluted formation water (0.5FW), or formation water (with varying salinities) and hydrochloric acid (HCl) in a specific ratio. This mixture was heated for three hours using an air-circulated oven and a hot plate with a magnetic stirrer. After heating, the solution is filtered through a 25 µm filter paper, yielding the biopolymer solution. The viscosity of this solution was then measured at different temperatures and shear rates using a Brookfield viscometer to evaluate the biopolymer's viscous behavior and properties. The details of polymer solution preparation and factors affecting yield and viscosity are previously discussed and presented in Ali et al. (Ali et al. 2024). Factors that determined the yield solution viscosity were investigated, as shown in **Table** 1**.**

Table 1. Investigated factors during polymer preparation.

Investigated Factors						
Water Salinity (ppm)	0 (DW)	37,000 (SW)	83,000 (0.5FW)	165,000 (FW)		
Peel Concentration (wt/L)	Powdered whole peel: 10%		2.5%,	5%,	7%,	8%,
	Crushed peel: 5%,		10%			
Heating Medium	Air Circulated	Hot Plate				
HCl Concentration (ml/L)	0	1	2.5	5	7.5	10
Peel Size	Crushed	Powdered				
Peel Part	Whole	Albedo				

Based on the concentration screening and injectivity considerations, the biopolymer formulation used for all corefloods in this study was prepared using SW (37,000 ppm), 5 mL/L HCl, and 7 wt/v powdered whole orange peels (heated on a hot plate with stirring). Solution viscosity was 24 cp at 25 ºC and 5.8 cp at 90 ºC, as shown in **Figure 1**. The biopolymer solution also showed shear-thinning behavior with increasing shear rate, as shown in **Figure 2.**

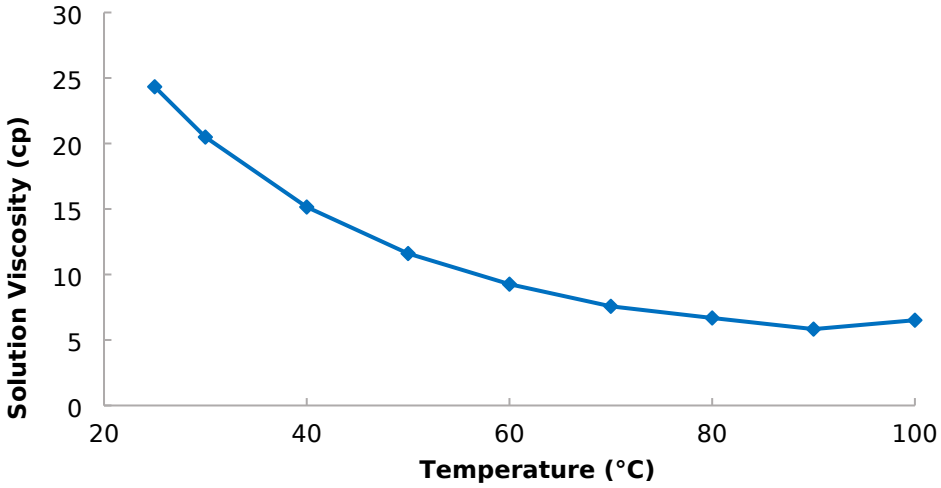

Figure 1. Apparent viscosity versus temperature for the citrus biopolymer solution prepared in synthetic seawater (TDS = 37,000 ppm).

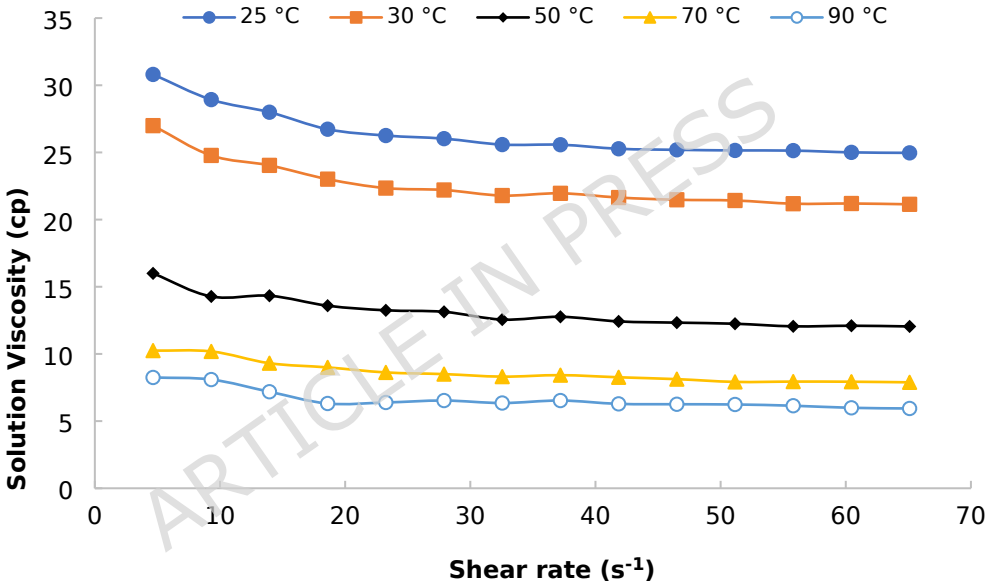

Figure 2. Apparent viscosity versus shear rate for the citrus biopolymer solution prepared in synthetic seawater (TDS = 37,000 ppm).

The apparent upturn in viscosity between 90 and 100°C is small relative to the overall decrease and is within expected measurement scatter at near-boiling temperatures. Possible contributors include increased measurement noise and minor solvent evaporation/concentration during high-temperature measurements. Importantly, the dominant trend is viscosity reduction with temperature, and the viscosity at 90°C (5.8 cP) remains the representative value used to discuss HSHT performance.

In this study, the oil-water and oil-biopolymer interfacial tension (IFT) were measured using a KRUSS K9 tensiometer; the results are reported in Section 3.2.

2.1.2 Concentration and preparation of synthetic water

Reservoir conditions were simulated by preparing synthetic FW and SW using a variety of salts, as outlined in (Ali et al. 2024). The FW was synthesized to replicate the composition reported for the Khafji field, based on unpublished field data. In parallel, SW with a total dissolved solids (TDS) level of 37,000 ppm was synthesized to represent the salinity of Arabian Gulf water. Both solutions were prepared in the laboratory by blending reagent-grade salt samples with a purity of greater than 99% with distilled water produced by a Gesellschaft Für Labortechnik (GFL 2008) water distillation unit.

2.1.3 Core samples and characterization

This research utilized core samples from two formations: Berea and Saq. Berea sandstone is internationally recognized for its use in experimental research, and Saq, a local sandstone formation in Saudi Arabia, has a relatively low clay content and high permeability compared to Berea samples. The Saq cores were obtained from outcrops in Qassim Province, and Berea sandstone was purchased from an international supplier in the United States. All cores are 1.5 inches in diameter. **Table** 2 shows the petrophysical properties of the core samples.

Table 2. Details of the used cores.

Formation	Core ID	Length (cm)	Diameter (cm)	Pore Volume (c^3)	Porosity (%)	Permeability (mD)
Berea	B10	12.3	3.81	27.11	19.3	160
	B9	11.4	3.81	24.8	19.3	154
	B8	12.9	3.81	31.4	21.3	100
Saq	Q12	5.7	3.81	16.47	25.34	130
	Q11	5.7	3.81	16.22	24.96	86

Q10	5.26	3.81	13.75	22.92	180

X-ray fluorescence (XRF) analysis was conducted to quantify the main elements for both Saq and Berea cores. The result showed that Berea sandstone is rich in Silica (Si), with lesser amounts of Aluminum (Al), Ferrite (Fe), and Potassium (K). In contrast, Saq sandstone has a higher silica content and lower Al, constituting the main elements. The XRF results are shown in **Table** 3.

Table 3. XRF Quantification for the used core samples.

Element	Saq (Mass%)	Berea (Mass%)
Si	94.66364	81.62211
Al	4.358373	7.986469
Ti	0.2272	0.560141
Ca	0.204284	0.34203
Fe	0.167911	6.196279
S	0.092068	0.01973
Zn	0.059576	0.042785
K	0.058282	2.818464
Mn	0.036714	0.131708
Cu	0.035299	0.070053
Ga	0.028553	0.019511
As	0.023279	0.034362
Cl	0.022261	0.019945
Sr	0.019485	0.019568
Zr	0.003074	0.116792

2.1.4 Characterization of the crude oil sample

Medium Saudi crude oil from Alkhafji fields was used (API of 26.88). The oil viscosity was measured at different temperatures (30, 50, and 80°C), yielding values of 27.59, 19.5, and 11.7 cP, respectively. The density of crude oil at different temperatures is shown in **Figure 3**.

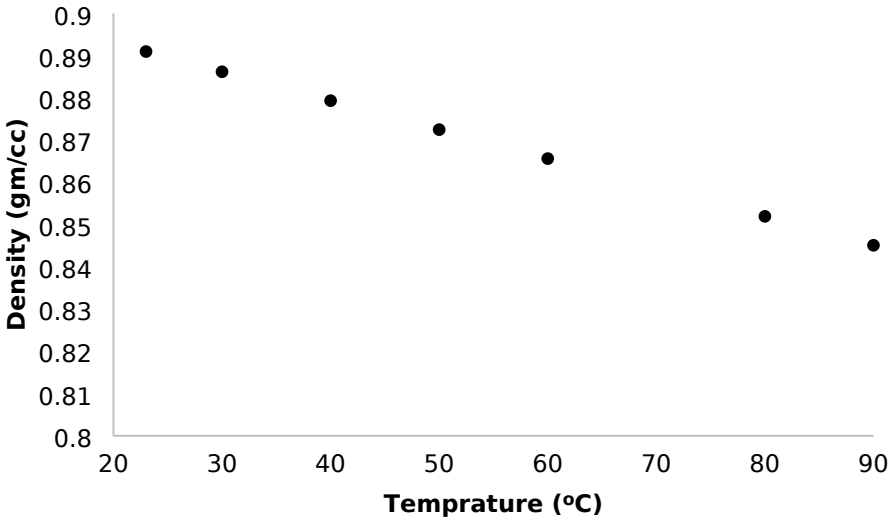

Figure 3. Density of crude oil at elevated temperatures.

2.2 Experimental setup and equipment

The density of the fluids was measured using Anton Paar DMA 5000, following standard measurement laboratory procedure. Also, surface and IFT of used fluids were measured using a KRUSS K9 tensiometer, where the IFTs between oil and water and between oil and polymer solutions were measured. The viscosity of the polymer solution was measured using a Brookfield LV DV-II+ viscometer. Additionally, Fourier Transform Infrared (FTIR) spectroscopy was conducted on the biopolymer solution to confirm the successful extraction of pectin, the primary viscosity-contributing component of the formulation. Moreover, a saturation unit that consisted of an air vacuum pump and a desiccator was used to saturate the core samples with FW.

Semi-automated core flooding system (CFS-200) was used to conduct core flooding experiments (**Figure 4**). The system is connected to two pumps; one was used to provide confining pressure, and the second was used to inject fluids into the cores. Both pumps can handle high pressure as required in the experiment. Three accumulators were connected to the core flooding system as fluid reservoirs for FW, SW, oil, and biopolymer solution. Heating tapes were used to maintain the selected temperature, covering all lines, core holders, and accumulators to keep the experiment temperature at the set value.

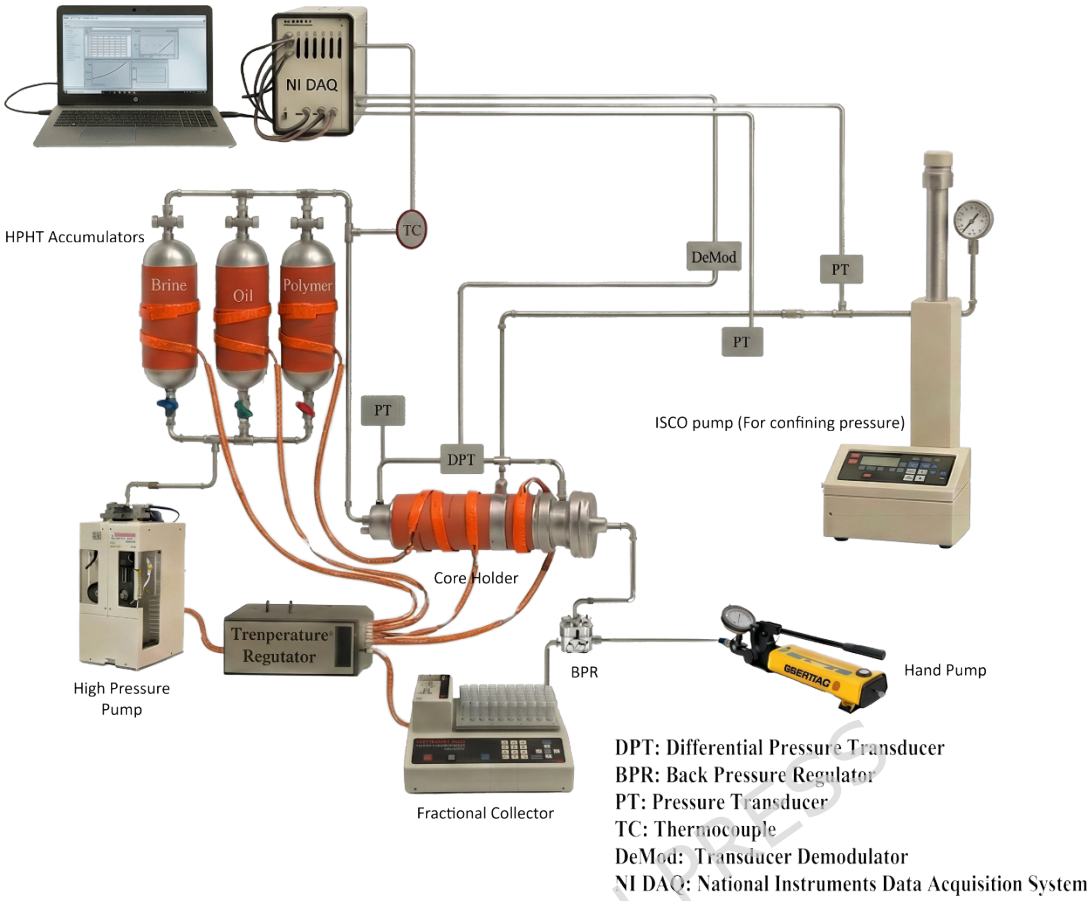

Figure 4. Schematic diagram of the core flooding system CFS-200 used for the experimental runs.

2.3 Experimental procedures

The solution preparation and characterization were presented in the previous research (Ali et al. 2024), where the extraction of the biopolymer procedures was discussed in detail. The cores used in the experiment were cut to lengths to fit the core flooding unit. They were then prepared for core flooding by drying at 70°C for 24 hours in the oven, followed by saturation in the saturation unit. Dimensions and weight of the cores were measured before saturation. Cores were saturated in a desiccator, which was connected to a vacuum pump and FW source. The vacuum pump was used to evacuate any air inside the cores and then saturated them with FW. The saturated weights of the cores were measured, and their pore volumes and porosity were calculated.

Next, the core flooding runs were conducted. First, the core flooding system was heated for 4 hours to attain a stabilized temperature of 90 ^{o}C.

Afterward, the FW was injected to establish 100% water saturation, and then permeability was measured at steady-state flow using four different flow rates. After that, the drainage process was performed on the cores, where the FW was displaced by crude oil at a flow rate of 0.5 cc/min. The volume of the expelled water was recorded to determine the initial oil saturation (S_{oi}). Then, the SW (displacing fluid) was added to the accumulator and left to achieve 90 ^{o}C. After which, flooding commenced according to the scenarios shown in **Table 4**.

Core flooding experiments were conducted using Berea sandstone samples (B8, B9, and B10) and Saq Formation core samples (Q10, Q11, Q12), as described in **Table** 2. The oil recovery (O.R.) was calculated after each core flooding phase to evaluate the effectiveness of the polymer and determine the optimal flooding scenario. Different pore volume (PV) of SW was used during seawater flooding (SWF) before and after water breakthrough (W_{BT}) to ensure 100% water cut (W_{cut}), while a polymer slug of 0.5 PV was always used during polymer flooding (PF).

Table 4. The different scenarios used for the Core flooding experiments.

# Run	Phase 1	Phase 2	Phase 3
1 (Base Case)	SW Injection till 100% W_{cut}	PF with 0.5 PV slug	SWF till 100% W_{cut}
2	SW Injection till W_{BT}	PF with 0.5 PV slug	SWF till 100% W_{cut}
3	PF with 0.5 PV slug	SWF Injection till 100% W_{cut}	

An important factor to consider during core flooding experiments is the resistance factor (F_R), which is a function of the pressure drop across the core during water flooding and after polymer injection, as shown in Eq. **Error! Reference source not found.**1). Another important factor is the residual resistance factor (F_{RR}), which is defined in Eq. **Error! Reference source not found.**2). They are key parameters in assessing the performance of polymer flooding (Thomas 2019; Gomaa et al. 2022).

$$F_R = \frac{\Delta P_p}{\Delta P_w} \quad (1)$$

$$F_{RR} = \frac{k_{wi}}{k_{wa}} \quad (2)$$

Where F_R is the resistance factor, F_{RR} is the residual resistance factor. ΔP_p is the pressure drop across the core after polymer flooding (in psi), and ΔP_w is the pressure drop across the core during water flooding (in psi). k_{wi} is the brine permeability before polymer flows through the core (in mD), and k_{wa} is the brine permeability after polymer flows through the core (in mD).

FR measures the effectiveness of polymer flooding in reducing mobility, while FRR quantifies the permeability reduction it causes. Both values remain above 1.0, which improves oil sweep efficiency. Elevated FR and FRR values indicate stronger potential for enhanced sweep efficiency and greater incremental oil recovery from polymer flooding. (Wang et al. 2018).

3. Results and Discussion

3.1 FTIR characterization of the biopolymer solution

FTIR spectroscopic analysis was performed to confirm the successful extraction of pectin from orange peels and to characterize the functional groups responsible for the biopolymer's viscosifying properties in EOR applications. The spectrum was acquired using transmission mode over the range of 4000-400 cm^{-1} with a resolution of 4 cm^{-1}. In **Figure 5**, the analysis showed characteristic absorption bands consistent with pectin structure, confirming the presence of the target biopolymer in the extracted solution.

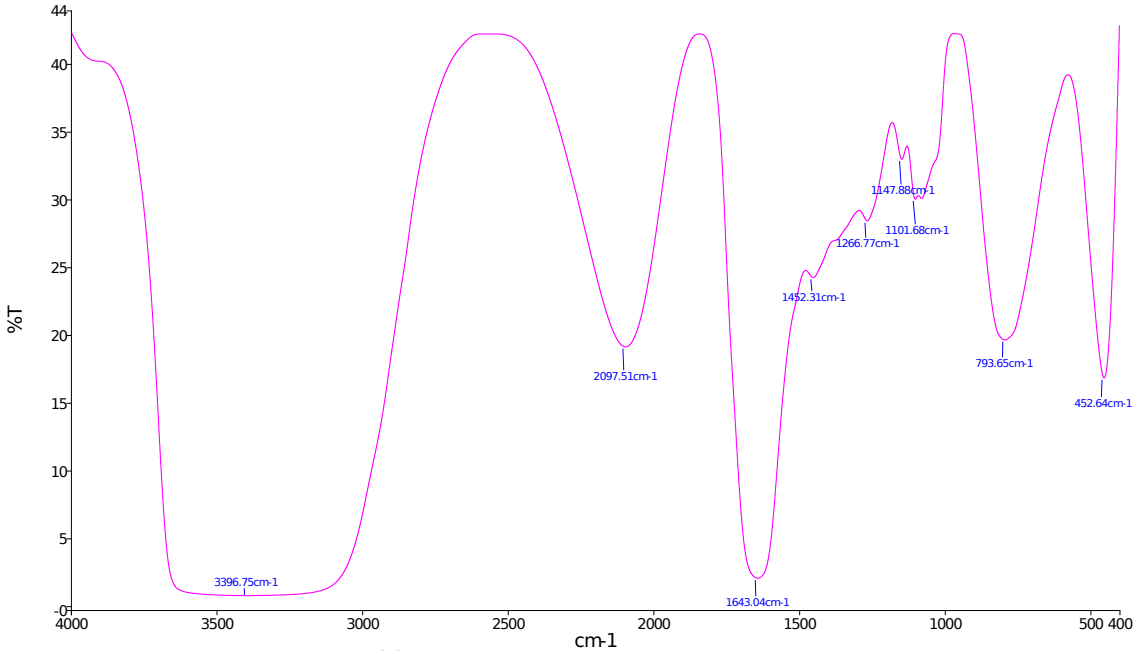

Figure 5. FTIR spectrum of the biopolymer solution.

The dominant feature in the spectrum was a broad O–H stretching band spanning ~3600–3100 cm−1 (centered near ~3397 cm−1), characteristic of hydrogen-bonded hydroxyl groups and bound water in polysaccharides, attributed to O-H stretching vibrations from pectin hydroxyl groups and hydrogen-bonded water molecules. This exceptionally strong and broad peak indicated the presence of extensive hydrogen bonding networks characteristic of hydrophilic polysaccharides, confirming the biopolymer's water-associating behavior, which is essential for viscosity enhancement in aqueous EOR formulations. A strong absorption at 1643 cm^{-1} corresponded to the asymmetric stretching vibration of carboxylate ions (COO^-), indicating partial ionization of the galacturonic acid carboxyl groups under the acidic extraction conditions. The corresponding symmetric COO^- stretching appeared at 1452 cm^{-1}. The frequency separation of 191 cm^{-1} between these bands suggested ionic interactions with the multivalent cations (Ca^{2+}, Mg^{2+}) present in the synthetic seawater, which is favorable for crosslinking and gel formation in high-salinity environments. The spectrum highlights the principal pectin-associated bands, including COO− asymmetric/symmetric stretching (1643 and 1452 cm−1) and glycosidic C–O–C/C–O bands in the 1200–1000 cm−1 region, supporting successful extraction of a pectin-rich, carboxylated biopolymer.

The C-O stretching vibration at 1267 cm^{-1} was diagnostic for the galacturonic acid backbone structure characteristic of pectin. This peak confirms the integrity of the α-1,4-linked galacturonic acid units that form the primary chain of pectin molecules. The polysaccharide backbone was further characterized by multiple C-O-C stretching and ring vibration modes, appearing at 1148, 1102, and 1080 cm^{-1}, which indicates the preservation of glycosidic linkages during extraction. Additional structural confirmation was provided by peaks in the fingerprint region at 794 and 453 cm^{-1}, which correspond to characteristic deformation modes of the pyranose ring system in galacturonic acid units. These low-frequency vibrations are specific to the pectin structure and support the identification of the extracted biopolymer.

Notably absent from the spectrum are the characteristic C=O ester stretching bands typically observed around 1740 cm^{-1} for methoxylated pectin, suggesting that the extraction conditions (elevated temperature, acidic pH, extended heating time) promoted de-esterification of the pectin. This results in a low-methoxyl pectin with predominantly free carboxyl groups, which is advantageous for EOR applications as it enhances ionic interactions with formation water components and improves gel stability in high-salinity environments. Additionally, an unexpected absorption band at 2098 cm^{-1} may be attributed to atmospheric CO_2 interference or residual compounds from the extraction process. This peak does not correspond to typical pectin functional groups and does not affect the overall structural identification.

The absence of characteristic cellulose absorption bands (1160, 1110, 1060, 1030 cm^{-1}) and lignin signatures (aromatic C=C stretching around 1510, 1460 cm^{-1}) confirms the selectivity of the extraction protocol in isolating pectin while removing unwanted plant cell wall components. The FTIR analysis conclusively demonstrated the successful extraction of pectin with a predominantly carboxylated structure, optimal for viscosity enhancement and ionic interactions required for effective EOR performance in high-salinity reservoir conditions.

3.2 Interfacial tension measurements

Oil-biopolymer IFT can influence capillary number and contribute to oil mobilization when reduced sufficiently. The measured IFT between the Saudi crude oil and synthetic seawater was 21.8 mN/m. Replacing SW with the used citrus-based biopolymer solution reduced the measured oil–aqueous IFT to 8.59 mN/m (60.6% reduction). This moderate IFT reduction is consistent with the presence of naturally occurring surface-active components in the waste-derived formulation; however, the IFT remains above the ultralow regime. Therefore, for the tested formulation, the coreflood incremental recovery is interpreted to arise primarily from mobility control (viscosity increase and increased flow resistance), with IFT reduction providing a secondary contribution.

It is worth noting that oil mobilization solely due to IFT reduction becomes pronounced when IFT is reduced below approximately 5 mN/m and approaches its maximum impact under ultralow IFT. Because the IFT measured for the current biopolymer formulation is 8.59 mN/m, the incremental oil recovery observed in the corefloods is attributed mainly to mobility control and sweep improvement.

3.3 Core flooding results

Alongside the oil recovery profiles, inlet and outlet pressures were recorded continuously during each run. Because all floods were performed at constant flow rate, step changes in ΔP ($\Delta P = P_{in} - P_{out}$) at stage switches (seawater → polymer → seawater) provide a direct indication of changes in flow resistance/apparent mobility within the core. In polymer stages, an increase in ΔP indicates increased resistance to flow relative to seawater, while a ΔP that remains elevated during the post-polymer seawater chase suggests residual resistance effects associated with polymer retention.

3.3.1 Biopolymer core flooding in Berea samples

Three core flooding experiments were conducted on Berea sandstone samples. In the first run, which serves as the base case, the core (B10) was initially fully saturated with FW, and then oil was injected to displace the FW. Subsequently, SW was injected until a 100% water-cut (W_{cut}) was achieved. Afterward, 0.5 PV of the extracted biopolymer was injected and displaced with SW. After SWF, the results demonstrated that the water breakthrough (W_{BT}) occurred after injecting about 0.5 PV of SW, and the O.R. was about 44.5% of OOIP. Additionally, the ultimate recovery rate after 100% of W_{cut} was 47.6%, as shown in **Figure 6**. The recorded pressure profile for the run is presented in **Figure 7**. The figure shows a relatively stable ΔP during the initial seawater flood, followed by a distinct step increase in inlet/outlet pressure and ΔP when the 0.5 PV biopolymer slug is injected. During the subsequent seawater chase, ΔP remains above the pre-polymer level, indicating that the flow resistance did not fully return to the initial waterflood condition. Despite this pressure response, the oil recovery curve **(Figure 6)** shows no incremental oil after polymer injection in this late-injection case, implying that polymer introduction at 100% W_{cut} increased resistance but did not improve macroscopic sweep in this Berea plug.

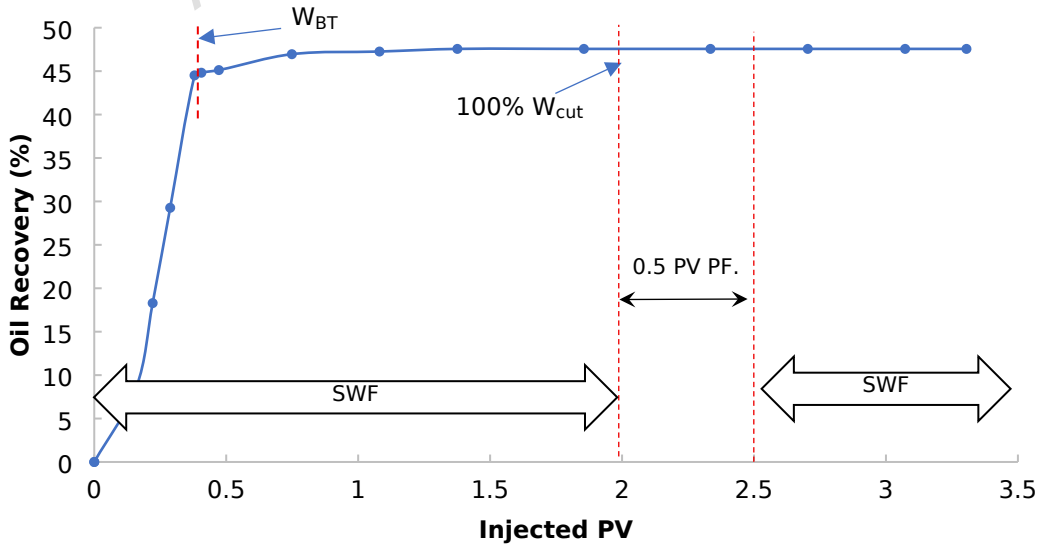

Figure 6. Oil recovery for the base run (B10).

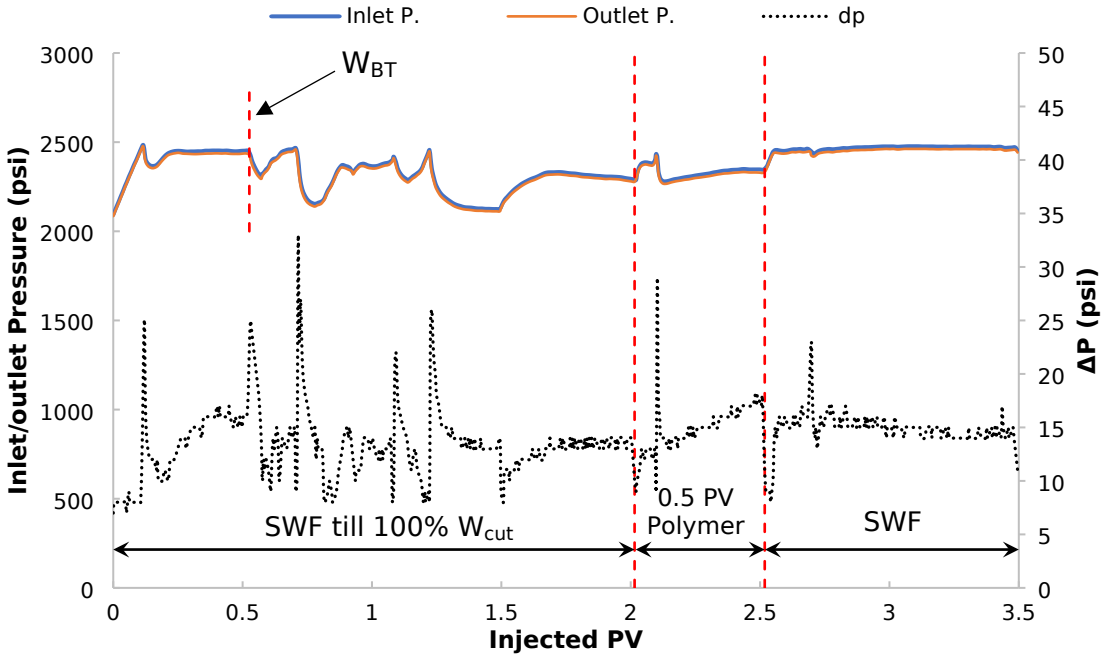

Figure 7. Pressure Profile for the base run (B10).

In the second run, the core (B9) was flooded by SW injection until reaching the W_{BT} phase. Next, 0.5 PV of the biopolymer was injected, followed by SWF until attaining a 100% W_{cut}. The results showed that the W_{BT} occurred after injecting approximately 0.45 PV of SW, and the O.R. was 41.5% at W_{BT}. In contrast, injecting 0.5 PV of the biopolymer yielded an additional 5.5% of OOIP. After the injection of 0.5 PV of biopolymer, SW flooding was conducted until a 100% water-cut was achieved, yielding a further 4.7% of OOIP in O.R. Additionally, the results indicated that the total O.R. was 51.7% of OOIP, as illustrated in **Figure** 8. The pressure profile of the second run is shown in **Figure** 9**.** The figure shows a clear ΔP increase during the polymer slug compared with the pre-breakthrough seawater stage. Unlike Run 1, polymer was injected immediately after W_{BT}, and the oil recovery profile (Figure 8) shows additional oil recovery during the polymer slug and subsequent seawater chase. The concurrent ΔP elevation and incremental oil indicates that mobility control occurred early enough to influence the displacement path before full water channeling developed.

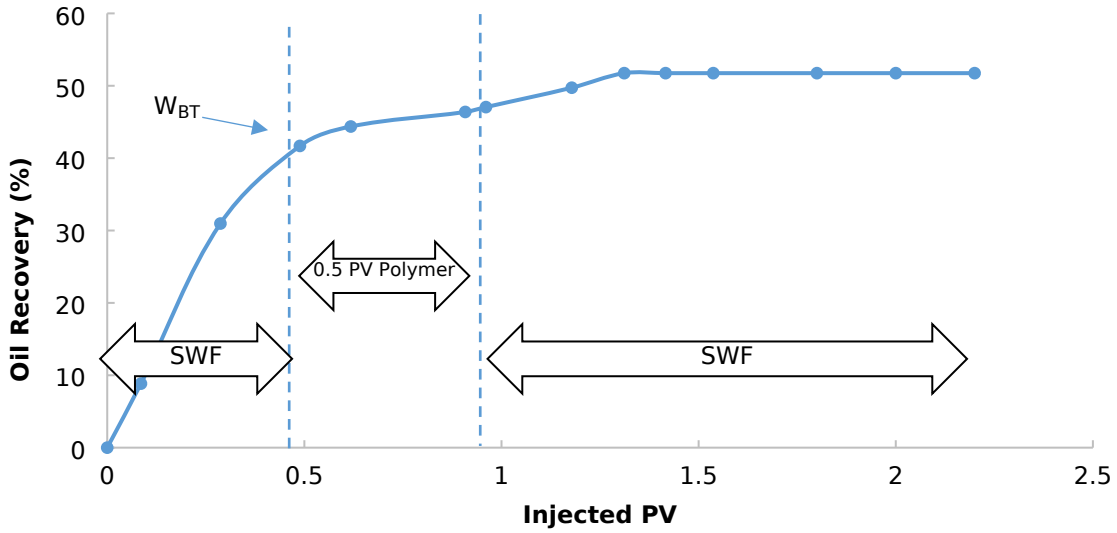

Figure 8. Oil recovery of the second run (B9).

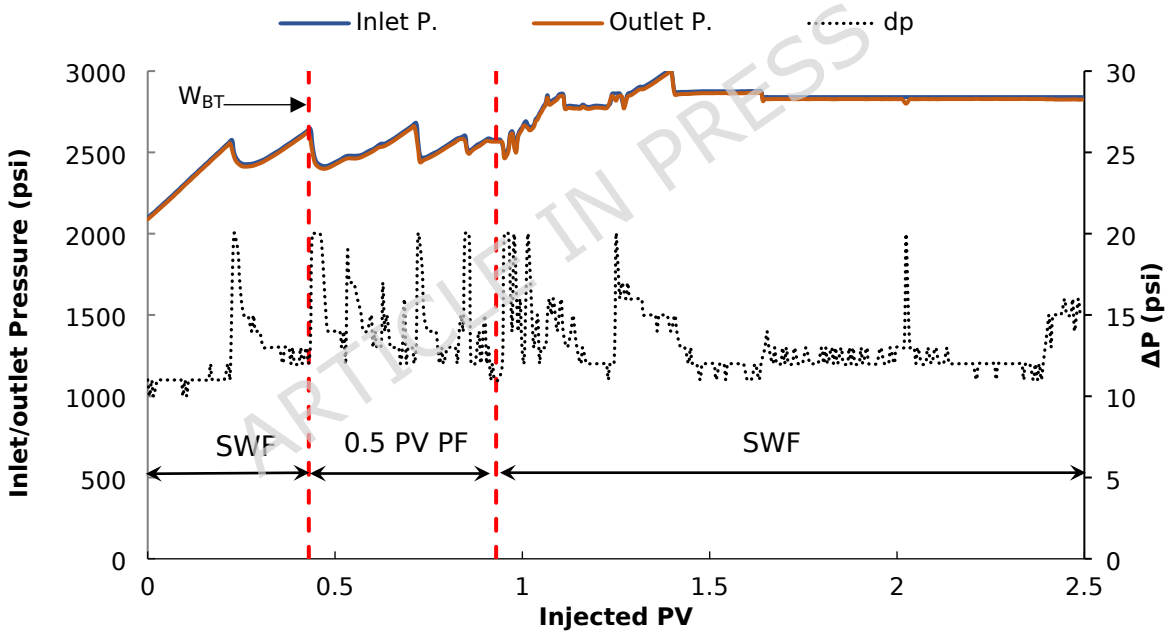

Figure 9. Pressure Profile of the second run (B9).

Using the third core sample (B8), the third run was performed. The biopolymer was injected much earlier than in the previous runs, where 0.5 PV of the biopolymer was injected initially, and then SW injection was performed until 100% W_{cut} was achieved. The results displayed that the W_{BT} occurred at a total injected volume of 0.55 PV (i.e., after ~0.05 PV of SW injection following the initial 0.5 PV polymer pre-slug), with a recovery rate of about 58.6% of the OOIP. Also, the results showed that injecting SW after

polymer yielded an ultimate recovery of 63.35% of OOIP, as shown in **Figure 10**.

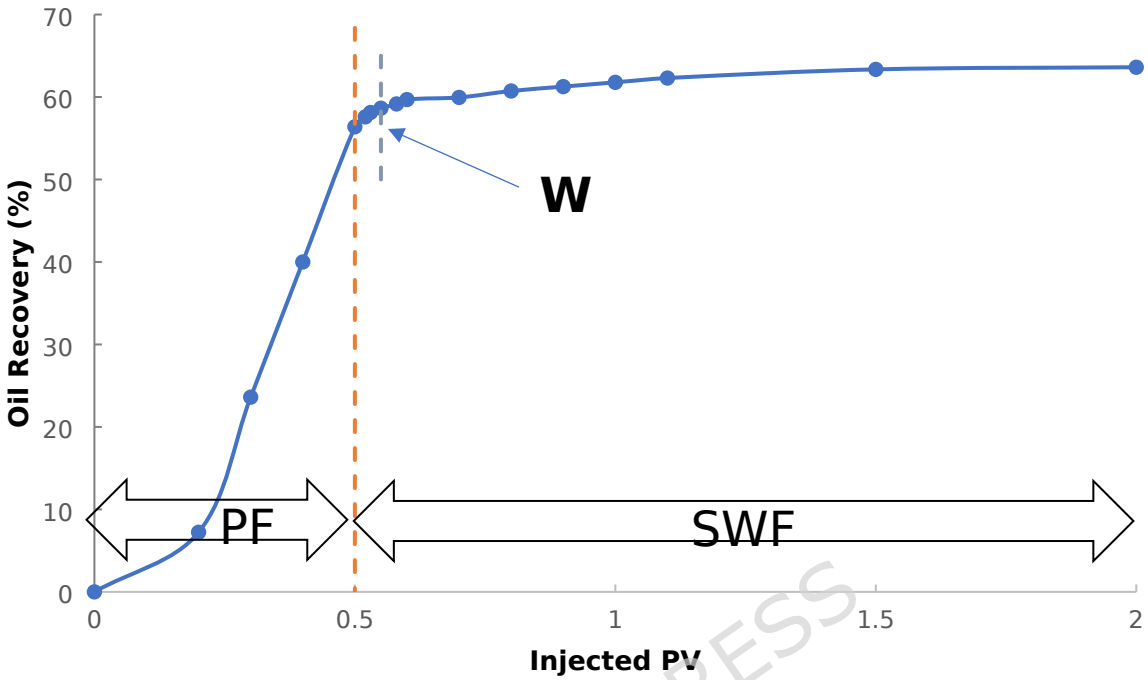

Figure 10. Oil recovery of the third run (B8).

Compared to the first and second runs, Run 3 yielded a higher O.R. because the biopolymer was present from the beginning of displacement (Figure 10). The pressure profile (Figure 11) shows that ΔP is elevated from the start of flooding and remains higher than in the late-injection cases, reflecting the higher flow resistance associated with polymer-controlled mobility during the early stages. This early ΔP elevation coincides with delayed WBT (0.55 PV) and a higher pre-breakthrough recovery, consistent with reduced early water channeling when mobility control is applied prior to seawater injection..

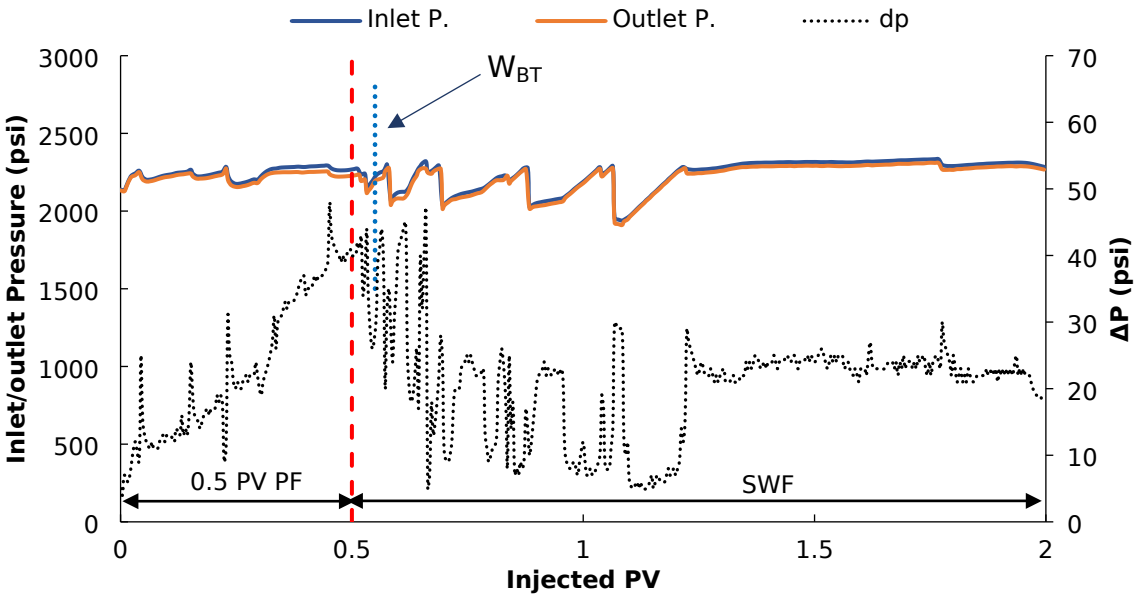

Figure 11. Pressure profile for the third run (B8).

Table 5 displays the summary of the O.R. for all runs using Berea core samples.

Table 5. Summary of oil recoveries from the Berea core samples based on the injection scheme and sequence.

Run	Injection	Injected PV @ W_{BT} (O.R. %)	Injection	O.R. %	Injection	Total oil R.%
1	SW	0.5 (44.5)	SW to 100% W_{Cut}	47.6	0.5 PV Polymer then SW	47.6
2	SW	0.45 (41.5)	0.5 PV Polymer	47	SW	51.7
3	0.5 PV Polymer	0.55* (58.6)	SW	--->	SW	63.35

* For Run 3, injected PV at WBT is reported as total PV (0.5 PV polymer + SW). The equivalent SW PV at W_{BT} is ~0.05 PV.

3.3.2. Biopolymer core flooding in Saq samples

Three core flooding experiments were conducted on the Saudi Saq sandstone formation. In the base case, the same scenario (**Table** 4) was done with the Saq samples. Core sample Q12 was used in this run, where the run started with SWF until a 100% W_{cut} was achieved. It is worth noting that at ~0.45 PV of SW, the W_{BT} was observed. The results showed that the O.R. at W_{BT} was about 35% of OOIP, and ultimate recovery was 46.2% of OOIP, as shown in **Figure** 12. The recorded pressure profiles of the inlet,

outlet, and ΔP are shown in **Figure** 13. Figure 13 shows that ΔP increased upon switching to the biopolymer slug after 100% Wcut, and ΔP remained elevated during the subsequent seawater chase. However, as shown by the oil recovery profile (Figure 12), no additional oil was produced after polymer injection in this late-injection case, indicating that the ΔP increase reflects increased flow resistance without a corresponding sweep improvement in the Saq plug under these conditions.

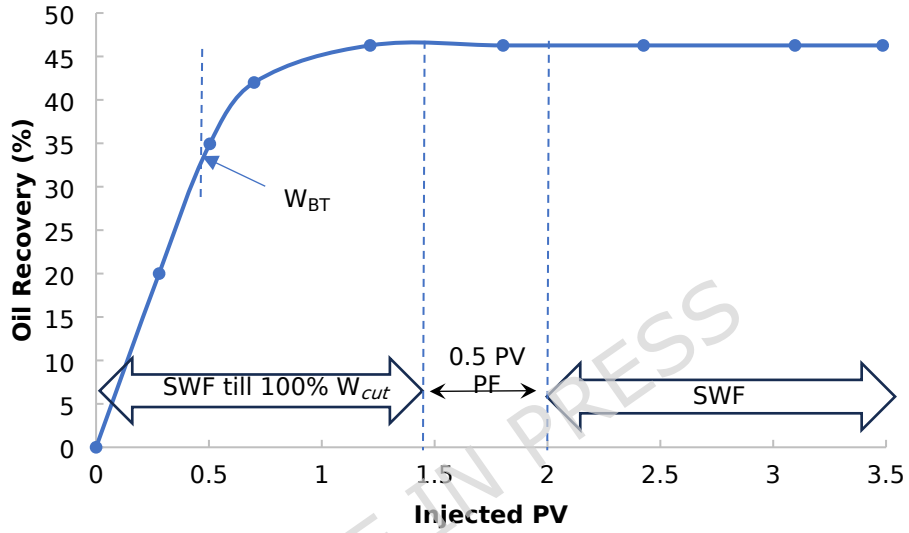

Figure 12. Oil recovery of the base run (Q12).

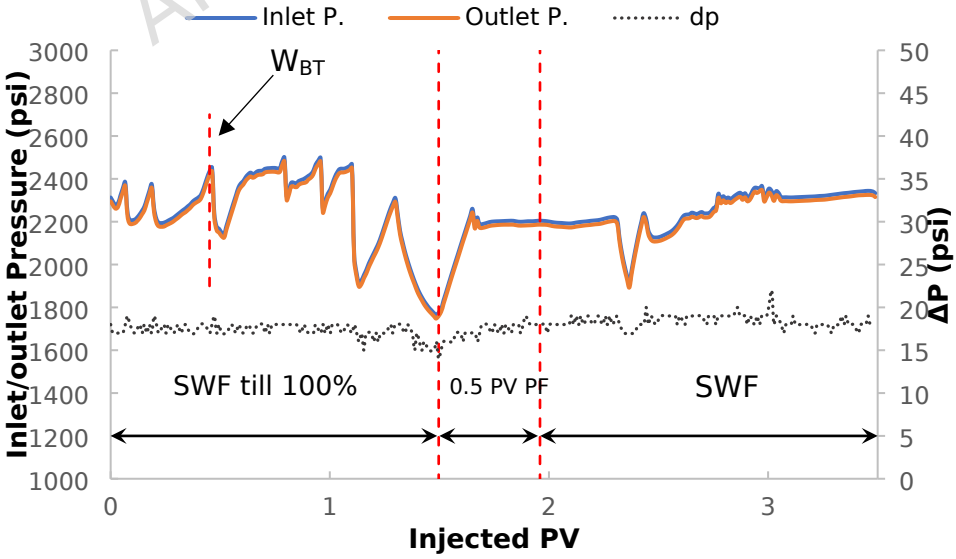

Figure 13. Pressure profile of the base run (Q12).

In the second run (core Q11), the SW was flooded only until W_{BT}. Then, 0.5 PV of the biopolymer was injected, followed by SWF until 100% W_{cut}. The results of this run showed that W_{BT} was observed after approximately 0.5 PV of SW injection, where the O.R. was 35.5% of OOIP (**Figure** 14). Afterward, injecting 0.5 PV of polymer yielded a 10% increase in O.R., resulting in a total of 46.5% OOIP. Compared to the results of the first run, total O.R. was similar to the ultimate oil recovery in the base case. The corresponding pressure profiles are presented in **Figure** 15. Consistent with the Berea experiments, the pressure profile for Run 2 in Saq (Figure 15) shows an increase in ΔP during the polymer slug relative to the pre-breakthrough seawater stage. Oil was produced during the polymer slug (Figure 14); however, the ultimate recovery at 100% Wcut (46.5%) showed very little increment compared to the base case (46.2%), suggesting that polymer injection after WBT in this Saq plug primarily accelerated recovery rather than increasing the final recovery."

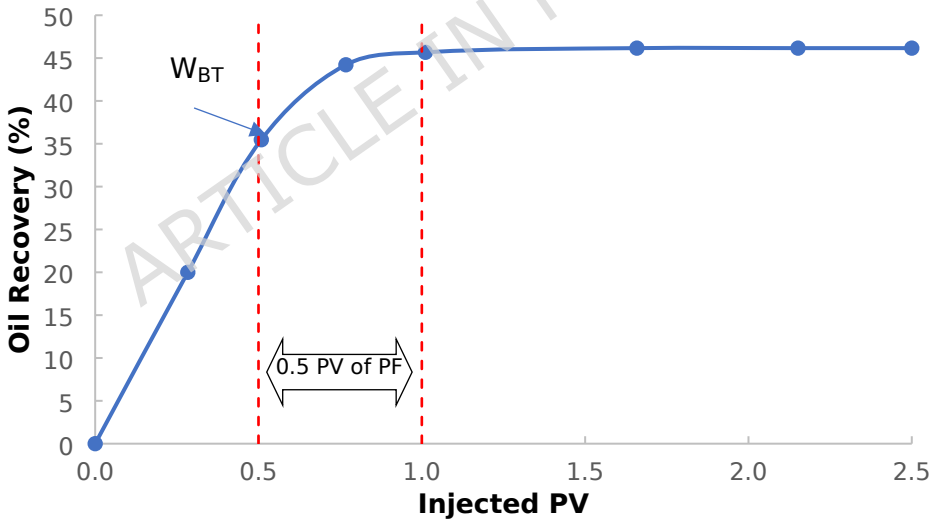

Figure 14. Oil recovery of the second run (Q11).

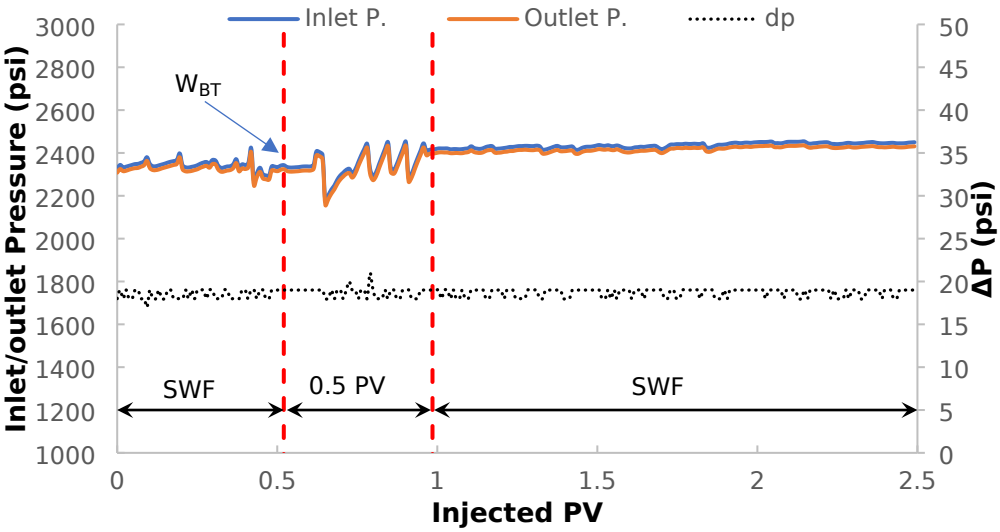

Figure 15. Pressure profile of the second run (Q11).

In the third run (core Q10), 0.5 PV of the biopolymer was injected, and the SW injection was conducted until a 100% W_{cut} was achieved. The results yielded a 26.12% recovery of OOIP (**Figure** 16). After injecting about 0.78 PV (0.5 PV of polymer and 0.28 PV of SW), W_{BT} was observed, and O.R. was 67.4% of OOIP. It is worth mentioning that injecting SW after polymer yielded an ultimate recovery of 70.3% of OOIP. The pressure profiles for this run are presented in **Figure** 17.

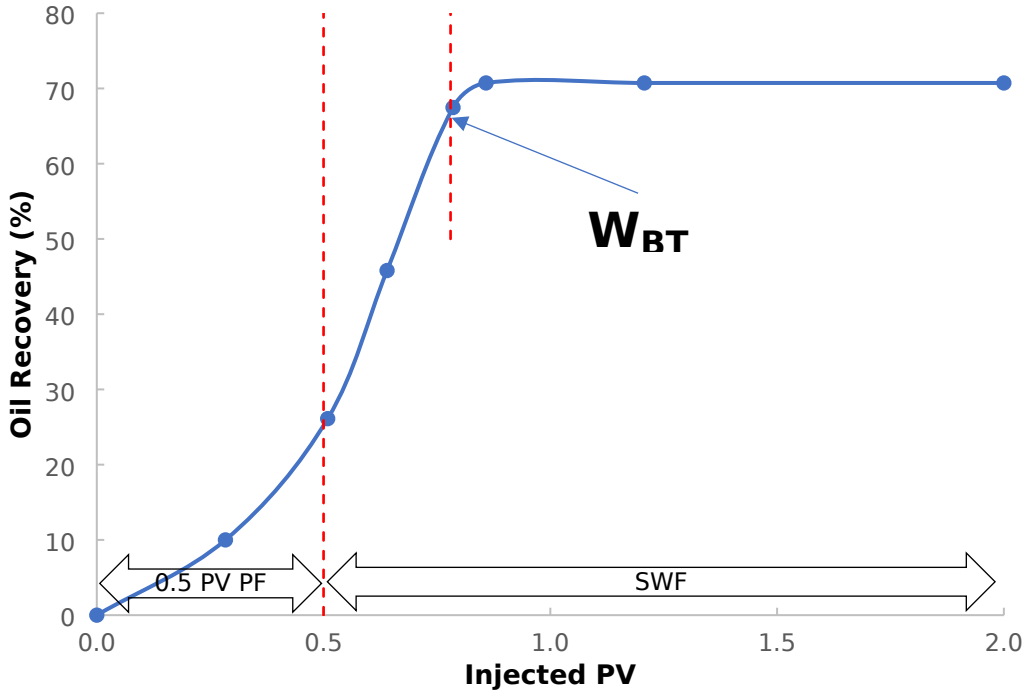

Figure 16. Oil recovery of the third run (Q10).

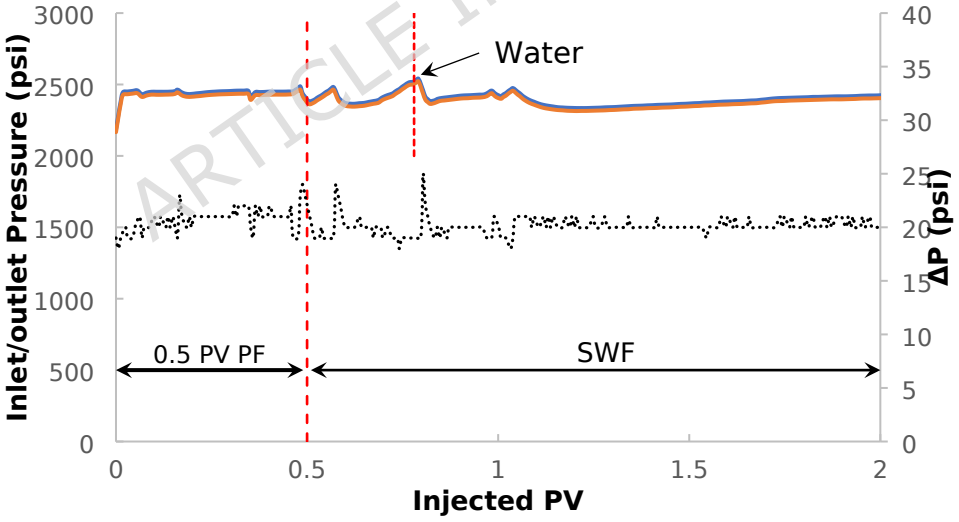

Figure 17. Pressure profile of the third run (Q10).

Table 6 shows the summary of the O.R. for all runs using Saq core samples.

Table 6. Summary of Saq core flooding experiments.

Run	Injection	Injected PV @ W_{BT} (O.R. %)	Injection	O.R. %	Injection	Total O.R.%
1	SW	0.45 (34.9)	SWF till 100% W_{cut}	46.2	0.5 PV PF followed by SWF	46.2
2	SW	0.5 (35.5)	0.5 PV Polymer	46	SW	46.5
3	0.5 PV Polymer	0.78 (67.5)	SW	--->	SW	70.3

3.4. Discussion

To interpret the pressure data, it is useful to recall that at constant injection rate the differential pressure across the core (ΔP) is inversely related to the apparent mobility of the injected phase. Therefore, the step increase in ΔP upon switching from seawater to the biopolymer slug in Figures 7, 9, 11, 13, 15 and 17 is expected for polymer flooding and corresponds to the resistance factor concept (Green and Willhite 2018; Levitt and Pope 2008; Thomas 2019). In several runs, ΔP did not return to the pre-polymer waterflood level during the seawater chase, which is commonly attributed to polymer retention/adsorption and associated residual resistance effects. Importantly, the present results show that a ΔP increase is necessary but not sufficient for incremental oil: the ΔP response must occur early enough to modify the displacement before dominant water channels develop, consistent with injection-timing studies (Juárez-Morejón et al. 2019; Shi et al. 2020; Zhu et al. 2020; Zhu et al. 2022).

3.4.1. Comparative analysis of the core flooding run #1 for both Berea and Saq samples

The results of water flooding for the first run (base case) for both Berea and Saq core samples were close to the reported result of water flooding by AlQuraishi et. al (AlQuraishi et al. 2019) who reported a 48.76% OOIP recovery using injection water with a salinity similar to that of the seawater used in this study (37,000 ppm). As shown in **Figure** 6 and **Figure** 12, the maximum O.Rs. for Berea and Saq cores were 47.6% and 46.2%,

respectively. After this stage, the injection of a 0.5 PV polymer slug did not increase the ultimate recovery.

However, the pore pressure increased after polymer injection, as shown in Figures 7 and 13. Switching from seawater to the 0.5 PV biopolymer slug produced a step increase in ΔP, and ΔP during the subsequent seawater chase remained higher than during the initial seawater flood. At constant injection rate, this behavior is consistent with reduced aqueous-phase mobility during polymer injection and residual resistance effects after the polymer slug (Green and Willhite 2018;Levitt and Pope 2008;Thomas 2019). Nevertheless, this pressure response did not translate to incremental oil in either core (Figures 6 and 12) because the waterflood had already established dominant aqueous flow paths by the time polymer was injected (100% Wcut). Consequently, the biopolymer likely propagated through these pre-existing water channels, providing limited additional sweep in these homogeneous plugs, consistent with injection-timing studies reporting diminishing incremental benefit when polymer flooding is initiated after stable water channels have formed (Thomas 2016;Juárez-Morejón et al. 2019; Shi et al. 2020)

3.4.2. Comparative analysis of the core flooding run #2 for both Berea and Saq samples

In the second core flooding scenario, when 0.5 PV of biopolymer was injected right after W_{BT} followed by SWF till 100% W_{cut}, a marginal increase in total O.R. for Saq sandstone was observed (46.2% to 46.5% OOIP; +0.3 percentage points), while for Berea sandstone, there was an incremental oil recovery of 4.1% higher than the first run (base case), as shown in **Figure** 18. There was a significant improvement in the percentage of oil recovered from residual oil after W_{BT} for Berea sandstone cores. The results showed that it increased from 5.6% to 17.44% of oil recovered from S_{or} after W_{BT} as shown in **Figure 19**.

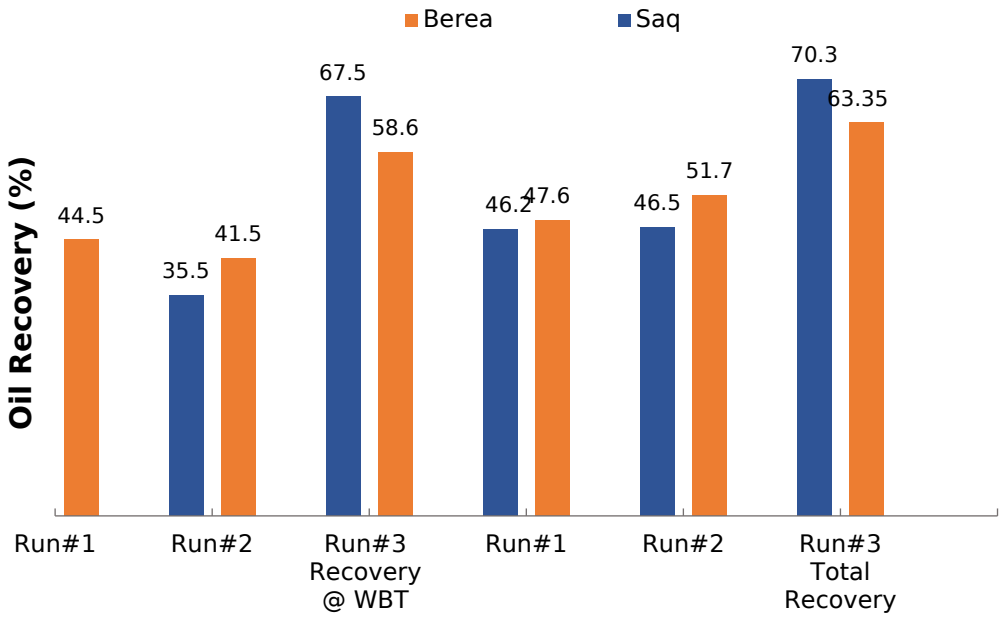

Figure 18. Comparison of the % OOIP recovered at W_{BT} and total O.R. for all runs scheme for both Berea and Saq core samples.

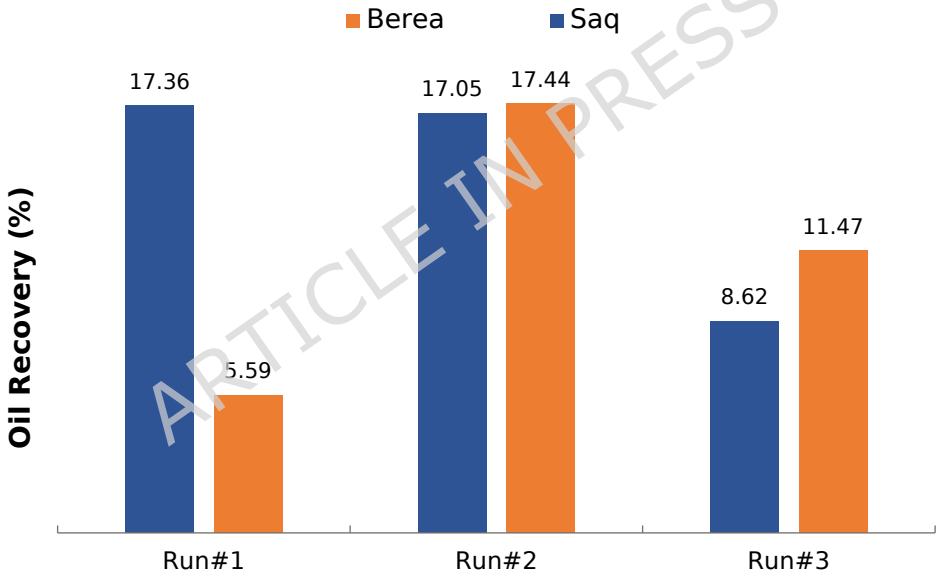

Figure 19. O.R. of residual oil after W_{BT} for Berea and Saq core samples.

Polymer injection timing plays a crucial role in recovery efficiency. In Run 2, introducing the biopolymer slug immediately after WBT led to a clear increase in ΔP relative to the base-waterflood in both cores (Figures 9, 15 and 20), consistent with the expected mobility reduction (FR>1) response in polymer flooding (Green and Willhite 2018;Levitt and Pope 2008;Thomas 2019). In Berea, the ΔP response coincided with an incremental recovery of 4.1% relative to the base case (Figure 18), indicating that mobility control

occurred early enough to partially influence sweep. In Saq, the ultimate recovery remained only marginally higher than the base case, indicating that under these conditions polymer injection mainly altered the recovery progression rather than the final recovery.

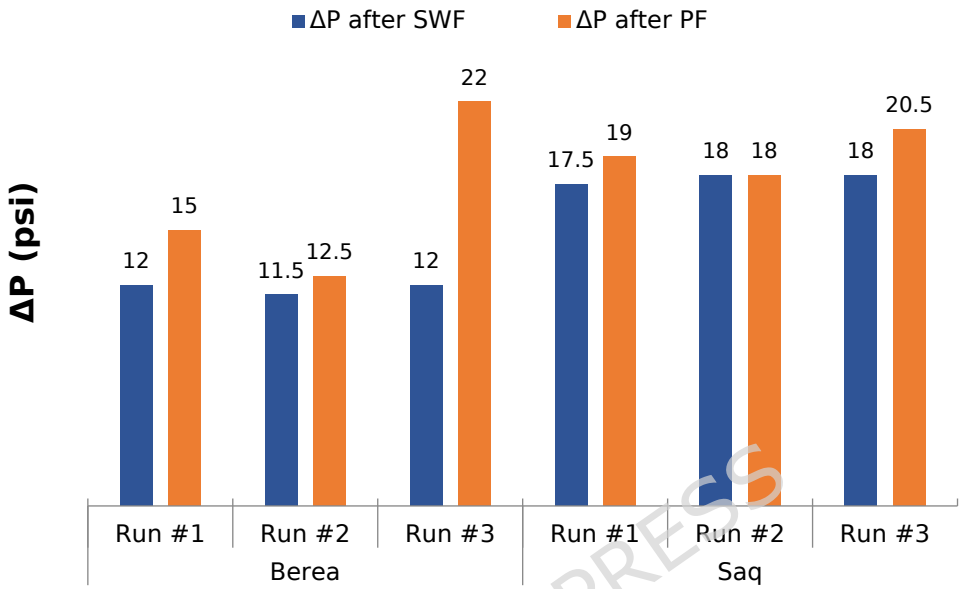

Figure 20. Comparison of changes in the observed ΔP due to polymer injection after initial SWF for all runs.

The ratio between ΔP during PF and ΔP during SWF suggests a higher resistance factor F_R (**Figure** 21), indicating a better sweep than water flooding. However, since polymer injection occurred after W_{BT}, the ultimate recovery showed only a slight improvement over the base case, as water had already established flow paths within the core, causing polymer fluid to follow these paths while moderately improving sweep efficiency, but not throughout the whole core.

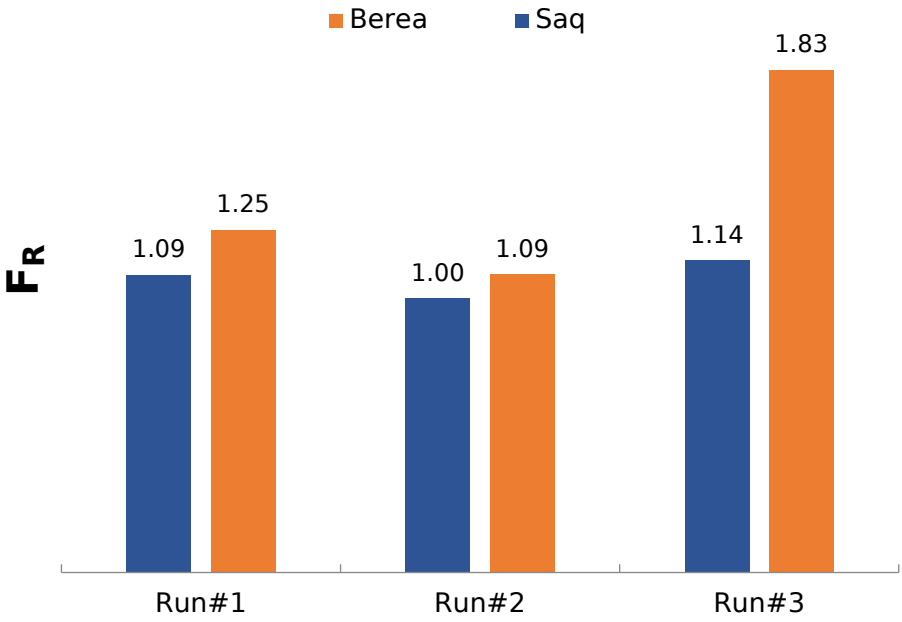

Figure 21. F_R for Berea and Saq sandstone for different injection scenarios.

These observations align with previous studies, which have shown that early polymer injection can significantly improve oil recovery by optimizing mobility control and reducing the volume of bypassed oil in reservoirs. According to (Shi et al. 2020), the optimal timing for polymer injection is typically just before W_{BT}, allowing the polymer to effectively manage flow in high-permeability zones and enhance sweep efficiency in low-permeability areas. Research indicates that initiating polymer flooding after a limited water injection can increase oil recovery by approximately 27.73% (Zhu et al. 2022), with the best results observed when the W_{cut} is maintained between 0% and 40% before polymer injection (Juárez-Morejón et al. 2019; Zhu et al. 2020).

3.4.3. Comparative analysis of the core flooding run #3 for both Berea and Saq samples

In the third injection scenario, 0.5 PV of the biopolymer was injected right at the beginning of the recovery stages prior to SWF, aiming to maximize the biopolymer effect and provide optimal sweep efficiency before W_{BT}. This approach resulted in significantly higher O.R. than the first and second runs, achieving up to 63% and 70% of OOIP for Berea and Saq

cores, respectively. These higher recoveries are likely due to enhanced sweep efficiency and an efficient (lower) mobility ratio, achieved by the spread of the polymer solution throughout the core, allowing for more areal sweeping before displacing the oil. As shown in the pressure profiles (Figures 11 and 17) and in the ΔP comparison (Figure 20), ΔP during the initial polymer stage (Run 3) was higher than in Runs 1 and 2, consistent with mobility control being applied before water channeling developed. Similar trends—higher early-time ΔP response accompanied by delayed WBT and increased recovery when polymer is injected early—have been reported in coreflood injection-timing studies (Ma et al. 2017; Juárez-Morejón et al. 2019; Sun et al. 2019;Shi et al. 2020)

As shown in **Figure** 20, the results revealed that the pressure difference after biopolymer injection increased, particularly during the third run when the polymer was injected before the SWF, indicating a negative effect on core permeability. The Saq core has a considerably higher permeability (180 mD) compared to the Berea core (100 mD). The higher permeability of Saq allows the viscous polymer solution to establish its flow path and corresponding pressure drop more rapidly across the core, leading to the observed early stabilization. Conversely, the lower permeability of the Berea core offers greater flow resistance, causing the pressure drop to build more gradually as the polymer progressively invades the pore space. These observations are evident in F_R values presented in **Figure 21.** The F_R values are higher for Berea cores, mainly in the third run. This suggests that the biopolymer is absorbed more extensively into the Berea core plugs compared to the Saq cores. Additionally, the XRF analysis (**Table 3**) showed that the Berea cores contain significantly higher amounts of Aluminum, Potassium, and Iron, indicative of a substantial clay content, compared to the cleaner, high-quartz Saq core. The higher clay content in the Berea cores might lead to more pronounced polymer adsorption and retention. This process progressively restricts flow paths as polymer injection continues, contributing significantly to the gradual increase in pressure drop seen in **Figure 11**. In contrast, the lower adsorption expected in the cleaner Saq core supports the stable pressure profile observed in **Figure**

17 after the initial polymer entry. As shown in **Figure** 21**,** higher F_R values of Brea support the analysis of the XRF results, which show higher silica in Saq than in Brea samples. Since the Saq cores are comparatively more silica-rich (quartz dominated); quartz surfaces are typically negatively charged at near-neutral pH, which can reduce adsorption of anionic, carboxylated polysaccharides such as low-methoxyl pectin via electrostatic repulsion; however, divalent cations may promote partial bridging. Therefore, differences in mineralogy and brine ionic strength can contribute to the observed differences in FR/FRR and pressure behavior between Berea and Saq cores. Moreover, the Saq Q10 core (5.26 cm) is substantially shorter than the Berea B8 core (12.9 cm). This shorter length allowed the polymer front to traverse the core and establish a stabilized flow condition much faster (relative to PV injected) compared to the longer Berea core.

As shown in **Figure** 22, a notable delay in W_{BT} was also observed, particularly in the Saq sandstone, occurring after injection of a total of 0.55 and 0.78 PV for Berea and Saq samples, respectively. The mechanism of enhanced recovery, as suggested by Shi et al. (Shi et al. 2020) proposes that in early polymer injection, the polymer creates a barrier in high-permeability zones, reducing water bypassing and enhancing oil recovery. This mechanism has been confirmed by multiple researchers, who demonstrated that early polymer injection improves sweep efficiency and optimizes polymer displacement capability, particularly in heterogeneous reservoirs, by preventing premature water breakthrough. Core flooding studies have confirmed that early polymer injection yielded an incremental recovery up to 15% higher than late injection scenarios (Ma et al. 2017; Juárez-Morejón et al. 2019; Sun et al. 2019).

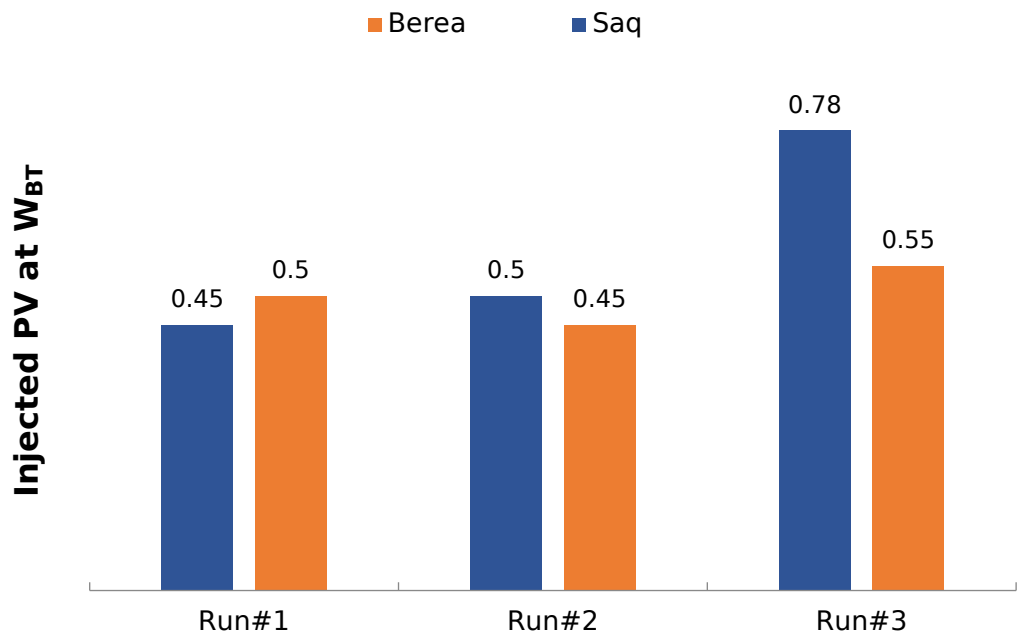

Figure 22. Delayed W_{BTs} after injecting polymer at an earlier stage are evident in Saq sandstone.

3.4.4 Sustainability and preliminary cost consideration

The proposed biopolymer is derived from orange peel waste generated by citrus-processing industries. Such waste streams are produced continuously where citrus is processed (e.g., juice production), and the peels can be dried and stored, reducing the impact of seasonality on supply. Valorization of this waste stream aligns with circular-economy principles and can reduce the environmental burden associated with synthetic polymer manufacture and disposal.

A preliminary laboratory-scale cost comparison (using laboratory-grade reagents and excluding capital and scale-up costs) indicates an estimated preparation cost of ~ $ 0.26 per liter of biopolymer solution, compared with ~ $ 0.27/L for laboratory-grade HPAM and ~$ 0.64/L for xanthan gum (Ali et al. 2024). Although laboratory-scale costs cannot be directly extrapolated to field scale, these values suggest cost-competitiveness relative to HPAM while providing biodegradability and waste-valorization benefits. Future work should provide a full techno-economic assessment at pilot/field scale.

3.4.5 Limitations and future work

The conclusions of this study should be interpreted in the context of the experimental scope and the practical constraints associated with HSHT coreflooding. Owing to the limited availability of intact, comparable core plugs and the time- and cost-intensive nature of high-temperature testing, each coreflood condition was performed as a single run per rock type. Accordingly, uncertainty associated with independent replicate experiments (e.g., standard deviations across repeats) is not reported, and the results are presented as trend-based comparisons of injection timing under consistent operating procedures. The use of comparatively homogeneous sandstone cores provides a controlled basis for mechanistic interpretation; however, reservoir-scale heterogeneity, gravity segregation, and larger-scale dispersion were not represented. Finally, while the biopolymer was injected at 90 °C; it didn't undergo an extended thermal aging or prolonged residence at 90 °C prior to injection; therefore, stability over field-relevant residence times warrants dedicated evaluation.

4. Conclusions

This study experimentally assessed a biopolymer derived from orange peel waste as a sustainable chemical EOR candidate for HSHT conditions. Corefloods in Berea and Saudi Saq sandstones demonstrate that injection timing strongly governs performance, with early placement providing the most consistent incremental recovery under the tested conditions. The pressure-response behavior supports mobility control and sweep improvement as the primary mechanism for the tested formulation.

- The formulated biopolymer (7 wt/v in synthetic seawater with 5 mL/L HCl) maintained an apparent viscosity of 5.8 cP at 90 °C and reduced oil–water IFT from 21.8 to 8.59 mN/m.
- Injection timing strongly affected recovery: pre-injection increased ultimate recovery from 47.6% to 63.35% OOIP in Berea and from 46.2% to 70.3% OOIP in Saq (incremental of ~15.8% and ~24.1% of OOIP, respectively).

- Polymer injection after water breakthrough provided incremental recovery relative to very late injection, whereas injection only at 100% water cut did not yield additional oil under the tested conditions. The ΔP responses and resistance factors indicate mobility control and sweep improvement as the dominant mechanisms; because the achieved IFT (8.59 mN/m) remains above the ultralow regime, IFT reduction is interpreted as a secondary contribution rather than the primary driver of mobilization.
- Valorization of orange peel waste offers a sustainability advantage aligned with circular-economy principles, and a preliminary laboratory-scale cost comparison (Ali et al. 2024) suggests potential cost-competitiveness with HPAM, motivating further scale-up and application-focused evaluation.

Acknowledgments

This work was supported by Ongoing Research Funding program, (ORF-2025-1408), King Saud University, Riyadh, Saudi Arabia. The authors thank the Department of Petroleum and Natural Gas Engineering for its support. The first author would like to thank the Dean of the Graduate School at King Saud University for funding his graduate education.

Funding Declaration

This work received no external funding.

Conflicts of Interest

The authors declare that they have no known competing financial interests or personal relationships that could have appeared to influence the work reported in this paper.

Author Contributions

Ammar Ali: Investigation, data curation, and writing; Abiodun Amao: Methodology, review, project administration, and editing; Faisal Altawati: validation, resources, writing – review & editing, visualization, project

administration, and funding acquisition; Taha Moawad: Conceptualization, methodology, review, project administration, and editing.

References

Aadland RC, Jakobsen TD, Heggset EB, et al (2019) High-Temperature Core Flood Investigation of Nanocellulose as a Green Additive for Enhanced Oil Recovery. Nanomaterials 9:665. https://doi.org/10.3390/nano9050665

Ahmadi Y, Ayari MA, Olfati M, et al (2023) Application of Green Polymeric Nanocomposites for Enhanced Oil Recovery by Spontaneous Imbibition from Carbonate Reservoirs. Polymers (Basel) 15:3064. https://doi.org/10.3390/polym15143064

Al Nabhani H, Al Riyami O, Al Sulaimani H, et al (2024) Use of Polymer Flooding to Enhance Oil Recovery from the Largest Oil-Bearing Clastic Reservoir in the South of the Sultanate of Oman. In: SPE Improved Oil Recovery Conference. Tulsa, Oklahoma, USA

Ali AG, Altawati FS, Elmahdy OA, et al (2025) Experimental Investigation of a Waste-Derived Biopolymer for Enhanced Oil Recovery Under Harsh Conditions: Extraction and Performance Evaluation. Polymers (Basel) 17:. https://doi.org/10.3390/polym17212896

Ali AG, Amao AM, Moawad TM (2024) Citrus-Based Biopolymer for Enhanced Oil Recovery Applications in High-Salinity, High-Temperature Reservoirs. Arab J Sci Eng 49:8643–8659. https://doi.org/10.1007/s13369-023-08619-6

AlQuraishi AA, Amao AM, Al-Zahrani NI, et al (2019) Low salinity water and CO2 miscible flooding in Berea and Bentheimer sandstones. Journal of King Saud University - Engineering Sciences 31:286–295. https://doi.org/10.1016/j.jksues.2017.04.001

Alvarado V, Manrique E (2010) Enhanced Oil Recovery: An Update Review. Energies (Basel) 3:1529–1575. https://doi.org/10.3390/en3091529

Chen Q, Wang Y, Lu Z, Feng Y (2013) Thermoviscosifying polymer used for enhanced oil recovery: rheological behaviors and core flooding test. Polymer Bulletin 70:391–401. https://doi.org/10.1007/s00289-012-0798-7

Clinckspoor KJ, Ferreira VH de S, Moreno RBZL (2021) Bulk rheology characterization of biopolymer solutions and discussions of their potential for enhanced oil recovery applications. CT&F - Ciencia, Tecnología y Futuro 11:123–135. https://doi.org/10.29047/01225383.367

Davison P, Mentzer E (1982) Polymer Flooding in North Sea Reservoirs. Society of Petroleum Engineers Journal 22:353–362. https://doi.org/10.2118/9300-PA

Divers T, Al-Hashmi AR, Al-Maamari RS, Favero C (2018) Development of Thermo-Responsive Polymers for CEOR in Extreme Conditions: Applicability to Oman Oil Fields. In: SPE EOR Conference at Oil and Gas West Asia. Society of Petroleum Engineers

Dupuis G, Antignard S, Giovannetti B, et al (2017) A New Thermally Stable Synthetic Polymer for Harsh Conditions of Middle East Reservoirs. Part I. Thermal Stability and Injection in Carbonate Cores.

Ekene DA, Nkechi NA, Uchechukwu ON, et al (2024) Experimental Investigation of the Suitability of Afzelia africana and Colocasian esculenta as Alternative to Hydroxyethyl cellulose in Enhanced Oil Recovery. Petroleum Science and Engineering 8:16–26. https://doi.org/10.11648/j.pse.20240801.13

Elsaeed ShimaaM, Zaki EG, Omar WAE, et al (2021) Guar Gum-Based Hydrogels as Potent Green Polymers for Enhanced Oil Recovery in High-Salinity Reservoirs. ACS Omega 6:23421–23431. https://doi.org/10.1021/acsomega.1c03352

Elsayed Abdel-Raouf M, Hasan El-Keshawy M, M.A. Hasan A (2022) Green Polymers and Their Uses in Petroleum Industry, Current State and Future Perspectives. In: Crude Oil - New Technologies and Recent Approaches. IntechOpen

Gaillard N, Sanders DB, Favero C (2010) Improved Oil Recovery Using Thermally And Chemically Protected Compositions Based On Co- And Ter-Polymers Containing Acrylamide. In: SPE Improved Oil Recovery Symposium. Society of Petroleum Engineers

Gao C (2016) Application of a novel biopolymer to enhance oil recovery. J Pet Explor Prod Technol 6:749–753. https://doi.org/10.1007/s13202-015-0213-7

Gao C (2015) Potential of Welan gum to enhance oil recovery. J Pet Explor Prod Technol 5:197–200. https://doi.org/10.1007/s13202-014-0135-9

Gbadamosi A, Patil S, Al Shehri D, et al (2022a) Recent advances on the application of low salinity waterflooding and chemical enhanced oil recovery. Energy Reports 8:9969–9996. https://doi.org/10.1016/j.egyr.2022.08.001

Gbadamosi A, Zhou X, Murtaza M, et al (2022b) Experimental Study on the Application of Cellulosic Biopolymer for Enhanced Oil Recovery in Carbonate Cores under Harsh Conditions. Polymers (Basel) 14:4621. https://doi.org/10.3390/polym14214621

Gomaa S, Soliman AA, Nasr K, et al (2022) Development of artificial neural network models to calculate the areal sweep efficiency for direct line, staggered line drive, five-spot, and nine-spot injection patterns. Fuel 317:123564. https://doi.org/10.1016/j.fuel.2022.123564

Green DW, Willhite GP (2018) Enhanced Oil Recovery. Society of Petroleum Engineers

Gunaji RG, Junin R, Bandyopadhyay S (2022) Application of biopolymer schizophyllan derived from local sources in Malaysia for polymer flooding operation. AIP Conf Proc 2541:60001. https://doi.org/10.1063/5.0127501

Haq B (2021a) Green Enhanced Oil Recovery for Carbonate Reservoirs. Polymers (Basel) 13:3269. https://doi.org/10.3390/polym13193269

Haq B (2021b) The Role of Microbial Products in Green Enhanced Oil Recovery: Acetone and Butanone. Polymers (Basel) 13:1946. https://doi.org/10.3390/polym13121946

Jang HY, Zhang K, Chon BH, Choi HJ (2015) Enhanced oil recovery performance and viscosity characteristics of polysaccharide xanthan gum solution. Journal of Industrial and Engineering Chemistry 21:741–745. https://doi.org/10.1016/j.jiec.2014.04.005

Jiang S, Lu W, Li T, et al (2024) Study on the Performance Mechanism of Polyformaldehyde Glycol Ether Polymer for Crude Oil Recovery Enhancement. Materials 17:437. https://doi.org/10.3390/ma17020437

Jiexun L, Zhongshan Z, Xuejun L, et al (2019) Polymer flooding technology in Daqing oilfield. Acta Petrolei Sinica 40:1104–1115. https://doi.org/10.7623/syxb201909008

Juárez-Morejón JL, Bertin H., Omari A., et al (2019) A New Approach to Polymer Flooding: Effects of Early Polymer Injection and Wettability on Final Oil Recovery. SPE Journal 24:129–139. https://doi.org/10.2118/190817-PA

Levitt DB, Pope GA (2008) Selection and screening of polymers for enhanced-oil recovery. Proceedings - SPE Symposium on Improved Oil Recovery 3:1125–1142. https://doi.org/10.2118/113845-ms

Li X, Xu Z, Yin H, et al (2017) Comparative Studies on Enhanced Oil Recovery: Thermoviscosifying Polymer Versus Polyacrylamide. Energy & Fuels 31:2479–2487. https://doi.org/10.1021/acs.energyfuels.6b02653

Li X, Yin HY, Zhang RS, et al (2019) A salt-induced viscosifying smart polymer for fracturing inter-salt shale oil reservoirs. Pet Sci 16:816–829. https://doi.org/10.1007/s12182-019-0329-3

Ma K, Li Y, Sun T (2017) Research and Practice of the Early Stage Polymer Flooding on LD Offshore Oilfield. J Pet Environ Biotechnol 08: https://doi.org/10.4172/2157-7463.1000337

Moawad TM, Elhomadhi E, Gawish A (2007) A Novel Promising, High Viscosifier, Cheap, Available and Environmental Friendly Biopolymer (POLYMTEA) for Different Applications at Reservoir Conditions Under Investigation. Part A: Polymer Properties. In: The Seventh Egyptian Syrian Conference on Chemical and Petroleum Engineering. Suez, Egypt

Muggeridge A, Cockin A, Webb K, et al (2014) Recovery rates, enhanced oil recovery and technological limits. Philosophical Transactions of the

Royal Society A: Mathematical, Physical and Engineering Sciences 372:20120320. https://doi.org/10.1098/rsta.2012.0320

Musa TA, Ibrahim AF, Nasr-El-Din HA, Hassan AnasM (2021) New insights into guar gum as environmentally friendly polymer for enhanced oil recovery in high-salinity and high-temperature sandstone reservoirs. J Pet Explor Prod Technol 11:1905–1913. https://doi.org/10.1007/s13202-020-01080-3

Nowrouzi I, Mohammadi AH, Khaksar Manshad A (2020) Characterization and likelihood application of extracted mucilage from Hollyhocks plant as a natural polymer in enhanced oil recovery process by alkali-surfactant-polymer (ASP) slug injection into sandstone oil reservoirs. J Mol Liq 320:114445. https://doi.org/10.1016/j.molliq.2020.114445

Obuebite A, Okwonna O (2023) Performance assessment of a novel bio-based polymer for enhanced oil recovery in high salinity sandstone reservoirs. GSC Advanced Research and Reviews 14:129–143. https://doi.org/10.30574/gscarr.2023.14.2.0061

Qi H, Liu Y, Shen S, Zhao J (2023) Green Polymer Poly-L-proline Efficiently Inhibits Formation of Gas Hydrates in Oil–Water System. Macromol Chem Phys 224:. https://doi.org/10.1002/macp.202300251

Seright RS, Wavrik KE, Zhang G, AlSofi AM (2020) Stability and Behavior in Carbonate Cores for New Enhanced-Oil-Recovery Polymers at Elevated Temperatures in Hard Saline Brines. SPE Reservoir Evaluation & Engineering 1–18. https://doi.org/10.2118/200324-pa

Sheng J (2011) Modern Chemical Enhanced Oil Recovery: Theory and Practice. Gulf Professional Publishing

Shi L, Zhu S, Guo Z, et al (2020) Experimental Study on the Effect of Polymer Injection Timing on Oil Displacement in Porous Media. Processes 8:93. https://doi.org/10.3390/pr8010093

Southwick JG, Driver JW, Dean RM, et al (2024) Optimizing Enhanced Oil Recovery: The Benefits of Preceding ASP and SP Floods with Polymer Flooding. In: SPE Improved Oil Recovery Conference. Tulsa, Oklahoma, USA

Standnes DC, Skjevrak I (2014) Literature review of implemented polymer field projects. J Pet Sci Eng 122:761–775. https://doi.org/10.1016/j.petrol.2014.08.024

Sun L, Li B, Jiang H, et al (2019) An Injectivity Evaluation Model of Polymer Flooding in Offshore Multilayer Reservoir. Energies (Basel) 12:1444. https://doi.org/10.3390/en12081444

Sveistrup M, van Mastrigt F, Norrman J, et al (2016) Viability of Biopolymers for Enhanced Oil Recovery. J Dispers Sci Technol 37:1160–1169. https://doi.org/10.1080/01932691.2015.1088450

Tackie-Otoo BN, Ayoub Mohammed MA, Mohamad Ghani MF, et al (2022) An Experimental Investigation into the Potential of a Green Alkali-

Surfactant-Polymer Formulation for Enhanced Oil Recovery in Sandstone Reservoir. In: Day 4 Fri, March 25, 2022. OTC

Tackie-Otoo BN, Ayoub Mohammed MA, Yekeen N, Negash BM (2020) Alternative chemical agents for alkalis, surfactants and polymers for enhanced oil recovery: Research trend and prospects. J Pet Sci Eng 187:106828. https://doi.org/10.1016/j.petrol.2019.106828

Tengku Mohd TA, Abdul Manaf SF, Abd Naim M, et al (2020) Properties of Biodegradable Polymer from Terrestrial Mushroom for Potential Enhanced Oil Recovery. Indonesian Journal of Chemistry 20:1382. https://doi.org/10.22146/ijc.52254

Thomas A (2019) Essentials of Polymer Flooding

Thomas A (2016) Polymer Flooding. In: Chemical Enhanced Oil Recovery (cEOR) - a Practical Overview. InTech

Vermolen ECM, Van Haasterecht MJT, Masalmeh SK, et al (2011) Pushing the envelope for polymer flooding towards high-temperature and high-salinity reservoirs with polyacrylamide based ter-polymers. SPE Middle East Oil and Gas Show and Conference

Wang C, Liu P, Wang Y, et al (2018) Experimental Study of Key Effect Factors and Simulation on Oil Displacement Efficiency for a Novel Modified Polymer BD-HMHEC. Sci Rep 8:3860. https://doi.org/10.1038/s41598-018-22259-z

Xie B, Liu X (2017) Thermo-thickening behavior of LCST-based copolymer viscosifier for water-based drilling fluids. J Pet Sci Eng 154:244–251. https://doi.org/10.1016/j.petrol.2017.04.037

Zhu S, Xue Z, Wang R, et al (2022) Experimental Study on Early Polymer Injection Timing of Heavy Oil Reservoir in Bohai Sea. Journal of Basic & Applied Sciences 18:140–146. https://doi.org/10.29169/1927-5129.2022.18.14

Zhu S, Ye Z, Zhang J, et al (2020) Research on optimal timing range for early polymer injection in sandstone reservoir. Energy Reports 6:3357–3364. https://doi.org/10.1016/j.egyr.2020.11.247